Jiao, Qunying

MACROSCOPIC NON-DESTRUCTIVE EVALUATION BY MODAL ANALYSIS TECHNIQUES

Iowa State University PH.D. 1986

PLEASE NOTE:

In all cases this material has been filmed in the best possible way from the available copy. Problems encountered with this document have been identified here with a check mark __✓__.

1. Glossy photographs or pages _____
2. Colored illustrations, paper or print _____
3. Photographs with dark background _____
4. Illustrations are poor copy _____
5. Pages with black marks, not original copy _____
6. Print shows through as there is text on both sides of page _____
7. Indistinct, broken or small print on several pages ✓
8. Print exceeds margin requirements _____
9. Tightly bound copy with print lost in spine _____
10. Computer printout pages with indistinct print _____
11. Page(s) _____ lacking when material received, and not available from school or author.
12. Page(s) _____ seem to be missing in numbering only as text follows.
13. Two pages numbered _____. Text follows.
14. Curling and wrinkled pages _____
15. Dissertation contains pages with print at a slant, filmed as received _____
16. Other _____

_____

_____

University
Microfilms
International

Macroscopic non-destructive evaluation by modal analysis techniques

by

Qunying Jiao

A Dissertation Submitted to the
Graduate Faculty in Partial Fulfillment of the
Requirements for the Degree of
DOCTOR OF PHILOSOPHY

Department: Engineering Science and Mechanics
Major: Engineering Mechanics

Approved:

Signature was redacted for privacy.

In Charge of Major Work

Signature was redacted for privacy.

For the Major Department

Signature was redacted for privacy.

For the Graduate College

Iowa State University
Ames, Iowa

1986

TABLE OF CONTENTS

	Page
NOMENCLATURE	viii
ABSTRACT	x
I. INTRODUCTION	1
A. The Problem	2
B. Literature Review	5
C. Objective	9
II. MODAL TESTING	12
A. Modal Testing	14
B. Parameter Estimation	24
C. Experimental Considerations for the Impact Method	29
III. EXPERIMENTAL PROCEDURES AND RESULTS	36
A. Experimental Set-up	36
B. Experimental Procedures	42
C. Experimental Results	46
D. Discussion	50
IV. FINITE ELEMENT MODEL	57
A. Introduction	57
B. Finite Element Results and Discussion	61
V. CONCLUSIONS AND RECOMMENDATIONS	74
A. Conclusions	74
B. Recommendations	76
VI. BIBLIOGRAPHY	78

VII. ACKNOWLEDGEMENT 81

VIII. APPENDIX A. MEASURED FREQUENCY RESPONSE FUNCTION 82

A. Measured Frequency Response Function of Plate with Various Horizontal Slot Lengths 82

B. Frequency Response Function Measured at Different Points on a Plate with Vertical Slot 84

IX. APPENDIX B. INPUT DATA SAMPLE 89

A. Input Data File 89

B. The Calculated Natural Frequencies 109

LIST OF FIGURES

		Page
Figure 1-1.	The trapezoidal plate	10
Figure 2-1.	Single degree of freedom model	15
Figure 2-2.	Single degree of freedom phase angle	16
Figure 2-3.	Linear system with input and output measurement noise	34
Figure 3-1.	Experimental apparatus	38
Figure 3-2.	The data acquisition system	39
Figure 3-3.	FRF measured using microphone	41
Figure 3-4.	FRF measured using accelerometer	41
Figure 3-5.	The measurement set-up	42
Figure 3-6.	Slot and measurement locations	43
Figure 3-7.	Measured coherence function for an undamaged plate	44
Figure 3-8.	Measured imaginary part of the FRF for a plate with a 3.0 in. slot at 45 degrees	45
Figure 3-9.	Measured real part of the FRF for a plate with a 3.0 in. slot at 45 degrees	45
Figure 3-10.	Frequency response function phase plot at measurement point No. 6 for 3 in. 45 degree slot	47
Figure 3-11.	Estimated modal shape for an undamaged plate	56
Figure 4-1.	Finite element mesh for an undamaged plate	59
Figure 4-2.	Finite element mesh for a plate with a 2.0 in. by 5/64 in. vertical slot	60
Figure 4-3.	The first five modal shapes of an undamage plate	69
Figure 4-4.	The first five modal shapes of a plate with a 2.0 in. vertical slot	72

Figure 4-5.	The first five modal shapes of a plate with a 3.0 in. 45 degree slot	74
Figure A-1.	Measured phase and magnitude of frequency response function of an undamaged plate	82
Figure A-2.	Measured phase and magnitude of frequency response function for a plate with a 2.0 by 5/64 in. horizontal slot	83
Figure A-3.	Measured phase and magnitude of frequency response function for a plate with a 2.5 by 5/64 in. horizontal slot	83
Figure A-4.	Measured phase and magnitude of frequency response function for a plate with a 3.0 by 5/64 in. horizontal slot	84
Figure A-5.	Phase and magnitude of frequency response function measured at point No. 1	85
Figure A-6.	Phase and magnitude of frequency response function measured at point No. 2	85
Figure A-7.	Phase and magnitude of frequency response function measured at point No. 3	86
Figure A-8.	Phase and magnitude of frequency response function measured at point No. 4	86
Figure A-9.	Phase and magnitude of frequency response function measured at point No. 5	87
Figure A-10.	Phase and magnitude of frequency response function measured at point No. 6	87
Figure A-11.	Phase and magnitude of frequency response function measured at point No. 7	88

LIST OF TABLES

		Page
Table 3-1.	Comparison of the natural frequencies measured using microphone and accelerometer	40
Table 3-2.	Measured natural frequencies of a plate with horizontal slot	48
Table 3-3.	Measured natural frequencies of a plate with 45 degree slot	48
Table 3-4.	Measured natural frequencies of a plate with vertical slot	49
Table 3-5.	Measured FRF phases for an undamaged plate	49
Table 3-6.	Measured FRF phases for a plate with a 3 in. vertical slot	50
Table 3-7.	Comparison of measured natural frequencies for three undamaged plates	51
Table 3-8.	Changes in the natural frequencies of a plate with a horizontal slot	52
Table 3-9.	Changes in the natural frequencies of a plate with a 45 degree slot	53
Table 3-10.	Changes in the natural frequencies of a plate with a vertical slot	54
Table 4-1.	Comparison of the natural frequencies of an undamaged plate with Maruyama's numerical result	62
Table 4-2.	Comparison between experimental and numerical results for natural frequencies of undamaged plates	63
Table 4-3.	Calculated natural frequencies of a plate with horizontal slot	63
Table 4-4.	Calculated natural frequencies of a plate with 45 degree slot	64
Table 4-5.	Calculated natural frequencies of a plate with vertical slot	64
Table 4-6.	Comparison of relative changes in the natural frequencies of a plate with a horizontal slot	65

Table 4-7. Comparison of relative changes in the natural frequencies of a plate with a 45 degree slot 65

Table 4-8. Comparison of relative changes in the natural frequencies of a plate with a vertical slot 66

Table 4-9. Comparison of relative changes in the natural frequencies for a 2.5 in. slot at three orientations 69

Table 4-10. Calculated natural frequencies of four plates with different slot widths 70

NOMENCLATURE

A_{jk}	modal constant
C	damping coefficient
D	flexural rigidity of plate
{D}	amplitude vector
E	Young's modulus
f_i	ith natural frequency
Δf_i	change of the ith order natural frequency
{f}	force vector
$G_{xx}(\omega)$	input auto-spectral density
$G_{yy}(\omega)$	output auto-spectral density
$G_{xy}(\omega)$	cross spectral density
h	thickness of the plate
$H(\omega)$	frequency response function
$H_{jk}(\omega)$	frequency response function measured at j with excitation at k
i	$\sqrt{-1}$
k	stiffness of spring
[K]	stiffness matrix
[δK]	change of the stiffness matrix
[M]	mass matrix
m(t)	input measurement noise
n(t)	output measurement noise
w(x,y,t)	transverse displacement of a plate
ρ	mass density

ω_r	estimated rth natural frequency
η	estimated relative damping factor
λ	eigenvalues
ν	Poisson's ratio
γ_{xy}	coherence function of x(t) and y(t)
$[\psi]$	modal shape matrix
$[\phi]$	normalized modal shape matrix

ABSTRACT

This dissertation describes an investigation of modal analysis methods for the detection, location, and characterization of flaws or damage in a structure or machine. The type of damage considered in the research was restricted to narrow, rectangular slots in symmetric trapezoidal plates. Both modal testing and finite element methods were used to investigate changes in natural frequencies of a clamped trapezoidal plate for all combinations of three slot lengths and three slot orientations. For modal testing, an impulse hammer was used to excite plate vibration, and a near field microphone was used to measure the response of the test plates. The first five natural frequencies were estimated from the measured frequency response function. Modal shapes associated with the natural frequencies were determined roughly from the phase of the measured frequency response function. Natural frequencies and associated modal shapes were also estimated numerically using the ADINA finite element package. Changes in natural frequencies for four different slot widths were investigated using finite element analysis. The changes in natural frequencies obtained by the two methods were in good agreement for all cases studied, and the results agree well with previously published work for an undamaged plate.

The investigation demonstrates that:

1. Slot presence can be detected from the change in natural frequency of the plate.
2. Slot length and angular orientation have significant effect on

natural frequencies of the plate.

3. Slot width has no significant effect on natural frequencies of the plates.
4. Slot presence can change the numerical order of the natural frequencies associated with adjacent modes of the plate.
5. Slot presence has little influence on modal shapes.

The results demonstrate that impact vibrational testing using a near field microphone as the response transducer is a viable method for macroscopic non-destructive evaluation.

I. INTRODUCTION

Non-destructive evaluation (NDE) consists of various methods to detect, locate, and characterize damage or flaws in a structure or machine. It is used to monitor and test the safety and soundness of structures or machines. Practically, there are always various types of flaws in a structure or machine. Depending upon the location, size, shape, and orientation of the flaws, some of the flaws may have little effect on the structure while others may cause failure of the structure or machine. In order to ensure the safety and integrity of a structure or machine, information about the existence, location, and characterization of the flaws is necessary.

In recent years, many new methods of NDE have been developed, including ultrasonic testing, radiography, eddy current methods, and acoustic emission. However, all existing methods have disadvantages as well as advantages, and there is no method that is universally applicable. One common disadvantage is that the components under inspection must be investigated in an exhaustive piece-wise manner. Thus, the time needed for inspecting large or complex structures is very long.

The modal testing method, measurement of the modal parameters including the natural frequencies and damping coefficients, is an attractive method for NDE. An advantage of the modal testing method is that the modal parameters can be measured at a single point on the structure and are relatively insensitive to the measurement location.

Moreover, the measured modal parameters can be used to evaluate the integrity of the structure. A disadvantage of this method is that it may be insensitive to the presence of small flaws or cracks that could cause failure of the structure or machine.

A. The Problem

The modal testing technique for NDE is based on the fact that modal parameters are global properties and are functions of the physical and geometrical parameters of the structure or machine. Therefore, any change in these physical or geometrical parameters will lead to changes in the modal parameters. On the other hand, measured changes in the modal parameters suggest changes in the physical or geometrical parameters of the structure. Thus, the measurement of modal parameters of a structure at two or more stages in its life provides an opportunity for the evaluation of the integrity of the tested structure. If modal parameters were measured before the structure was put in service, subsequent measurements of the parameters can be used to estimate changes in the structure's properties, and to estimate the continuing soundness of the structure.

Theoretically, any change in physical or geometrical parameters of the structure or machine would cause changes in the stiffness. The influence of damage or a flaw on the stiffness of a structure can be modelled by introducing a small change in the stiffness matrix of the structure. The equation of motion for free vibration of a multi-degree of freedom system is

$$[K]\ \{D\} = \lambda[M]\ \{D\} \qquad (1\text{-}1)$$

where, [K] is the stiffness matrix

$\{D\}$ is the amplitude vector

[M] is the mass matrix

and λ is the eigenvalue.

For small changes in the mass and stiffness matrices [δK] and [δM], there will be a small change in the amplitude vector {δD}. Thus, the equation of motion for the modified system is

$$([K]+[\delta K])(\{D\}+\{\delta D\}) = (\lambda+\delta\lambda)([M]+[\delta M])(\{D\}+\{\delta D\}) \qquad (1\text{-}2)$$

Neglecting second order terms in Eq. (1-2) results in the linearized equation

$$([\delta K] -\delta\lambda[M]-\lambda[\delta M])\{D\} + ([K]-\lambda[M])\{\delta D\} = 0 \qquad (1\text{-}3)$$

Multiplying both sides of Eq. (1-3) by $[D]^T$ gives

$$\{D\}^T([\delta K]-\delta\lambda[M]-\lambda[\delta M])\{D\} + \{D\}^T([K]-\lambda[M])\{\delta D\} = 0 \qquad (1\text{-}4)$$

The mass matrix [M] and the stiffness matrix [K] are symmetric matrices, so that the transpose of Eq. (1-1) is

$$\{D\}^T([K] -\lambda[M]) = 0 \qquad (1\text{-}5)$$

Substituting Eq. (1-5) into Eq. (1-4), it becomes

$$\{D\}^T([\delta K] - \delta\lambda[M] - \lambda[\delta M])\{D\} = 0 \qquad (1\text{-}6)$$

For most types of structural damage, the change in the mass matrix is much smaller than the change in stiffness or displacement matrices and can be neglected. Equation (1-6) thus becomes

$$\{D\}^T([\delta K] - \delta\lambda\,[M])\{D\} = 0 \qquad (1\text{-}7)$$

and solving for the change in eigenvalues gives

$$\delta\lambda = \frac{\{D\}^T\,[\delta K]\,\{D\}}{\{D\}^T\,[M]\,\{D\}} \qquad (1\text{-}8)$$

Equation (1-8) relates the change in the eigenvalues to the change in the stiffness matrix. In this equation, the displacement vector {D} and mass matrix [M] are associated with the undamaged system, and can be obtained experimentally or numerically. Therefore, the changes in natural frequency $\delta\lambda$ can be determined by measuring the natural frequencies of the damaged structure. Equation (1-8) can be used to estimate the change in stiffness [δK], provided that {D}, [M], and $\delta\lambda$ are known.

B. Literature Review

Modal testing for NDE is a relatively new field in which little work has been done. In this section, a summary of existing damage detection techniques that are based upon experimental mechanical vibration methods will be examined.

The earliest work involving vibration techniques for non-destructive evaluation was reported in 1978 by Adams et al. [1]. They began with an investigation of one dimensional components including a straight prismatic bar and an automobile camshaft. They modelled one dimensional problems using the receptance analysis method. By measuring the natural frequencies at two or more stages of increasing damage, they successfully detected and located damage in one dimensional components. However, the method cannot be used to solve two dimensional problems because there is no receptance technique for two dimensional problems. For this reason, they used finite element analysis to study the change in natural frequencies of two rectangular plates [2]. In the two dimensional problem, they related the change in natural frequency to the change in stiffness of the plate. They also carried out an experimental study using two different plates. The plates were excited by a loudspeaker, while the response signals were measured using strain gages. The modal shapes were checked roughly by spreading sand over the surface of the plate undergoing excitation. The changes in the natural frequencies were measured for a rectangular hole and saw-cut slot. They concluded that the presence of damage can be determined from the change in natural frequency, but the location and estimation of the severity of

the damage require dynamic analysis.

Crema, Castellani, and Peroni [3] investigated the possibility of damage detection in a fiber glass blade of a small windpower turbine using modal analysis methods. They measured changes in the natural frequencies and compared the experimental data with finite element results. They found that the results agreed well for a large number of vibration modes. They also tried to measure changes in damping coefficients, but the results were inconclusive. They concluded that high frequency resolution and zoom techniques are necessary to evaluate changes in natural frequencies and damping coefficients precisely.

Tracy, Dimas, and Pardoen [4] used modal analysis techniques to study the effects of impact damage in composite plates. They argued that for surface damage, modal testing works better than either ultrasonic C-scan or radiography. In their modal testing procedure, a broadband white noise signal was fed to an electromagnetic shaker that excited the plate. A small accelerometer was used to measure the response. In order to identify the natural frequency, damping coefficient, and modal shapes, the measured frequency response functions were curve-fit to yield the modal parameters. They corroborated the measured data with finite element analysis. They also found good agreement between numerical and experimental results, and found that the experimental modal shapes are closer to the numerical modal shapes at lower frequencies.

Chondros and Dimarogonas [5] studied the influence of a crack on the dynamic behavior of a structural member. They developed a

cantilever beam model for welded joints. They also investigated, both analytically and experimentally, the relationship between the change in natural frequencies of a cantilever beam and the depth of a transverse crack located at the built-in end of the beam. They argued that the modal analysis method can be applied more easily than any other method to large structures in the field. They also noted that the method is less sensitive to small cracks than other methods such as ultrasonic scanning.

Yang, Chen, and Dagalakis [6] successfully used a random decrement technique to predict four different levels of damage in a model of an offshore structure. Random decrement techniques are based on the decomposition of the random response of a structure into deterministic and random components. By averaging over a large number of samples of the same response, the random component is averaged out, and the deterministic component, which is the free-decay response of the system under random loading, remains. The advantage of this technique is that only measurements of the dynamic response of the structure are required. The input excitation causing the response need not be measured. They concluded that the random decrement technique was able to distinguish between damage and non-damage situations using only four accelerometers mounted an each of the legs of the structure.

Gudmundson conducted a series of analytical studies of the dynamic behaviour of structures with different forms of cross-sectional cracks. In 1982 [7], he derived an equation to predict the changes in the natural frequencies of a structure with different length cracks using

the first perturbation method. His equation shows that the change in natural frequency due to a crack depends on the strain energy of a static solution. The method has been tested for three different cases, and the predicted results correlate with experimental results for small cracks. In 1983 [8], Gudmundson improved his previous work by using a consistent static flexibility matrix to model the crack. This mathematical model was applied to an edge-cracked cantilever beam. The validity of the present model was confirmed by comparisons with experimentally obtained natural frequencies for the same beam. In 1984 [9], based on his previous work, he developed an analytical expression for determination of the changes in natural frequencies and damping due to small cracks. He also derived an equation to predict the length, position, and orientation of a crack using the measured frequency changes.

It is clear from the foregoing that most of the published work in this area deals with one dimensional problems. Little work has been reported for two dimensional situations. For one dimensional problems, a number of methods for detecting and locating flaws or damage have been developed. For two dimensional problems, the presence of damage or flaws can be determined from changes in the natural frequencies of a structure. However, methods for locating and characterizing the damage have yet to be established. Thus, further systematic work in this direction is necessary.

C. Objective

The primary purpose of this project is to locate and characterize damage or flaws in a two dimensional structure by modal analysis techniques. In the research described here, the effects of the dimensions and orientation of damage on changes in the natural frequencies of a clamped trapezoidal aluminum plate are investigated using modal testing and finite element methods. Figure 1-1 is a sketch of the particular trapezoidal plate geometry that was investigated. Damage is simulated by cutting slots of different sizes and orientations into the center of the plate. The length, width, and angular orientation of the slot are changed. The slot length considered ranges from 2.0 to 3.0 inches, while the slot width ranges from 0.02 to 0.17 inches. Three slot orientations of 0, 45, and 90 degrees with respect to the base of the trapezoidal plate are considered. The natural frequencies for the undamaged and damaged plates are determined. The effects of slot width, length, and orientation on changes in the natural frequencies of the plate are studied.

The dimensions of the test plate are the same as was used by Maruyama, Ichinomiya, and Narita [10]. Maruyama and coworkers used the real time method of time averaged holographic interferometry to measure the natural frequencies and modal shapes of a trapezoidal plate. They also compared their experimental results for the natural frequencies and modal shapes with numerical predictions. The comparison revealed errors of less than 6% and an average error of 3.6%. Their results provide a good reference for experimental and finite element analysis, and it was

for this reason that the trapezoidal plate was chosen for this investigation.

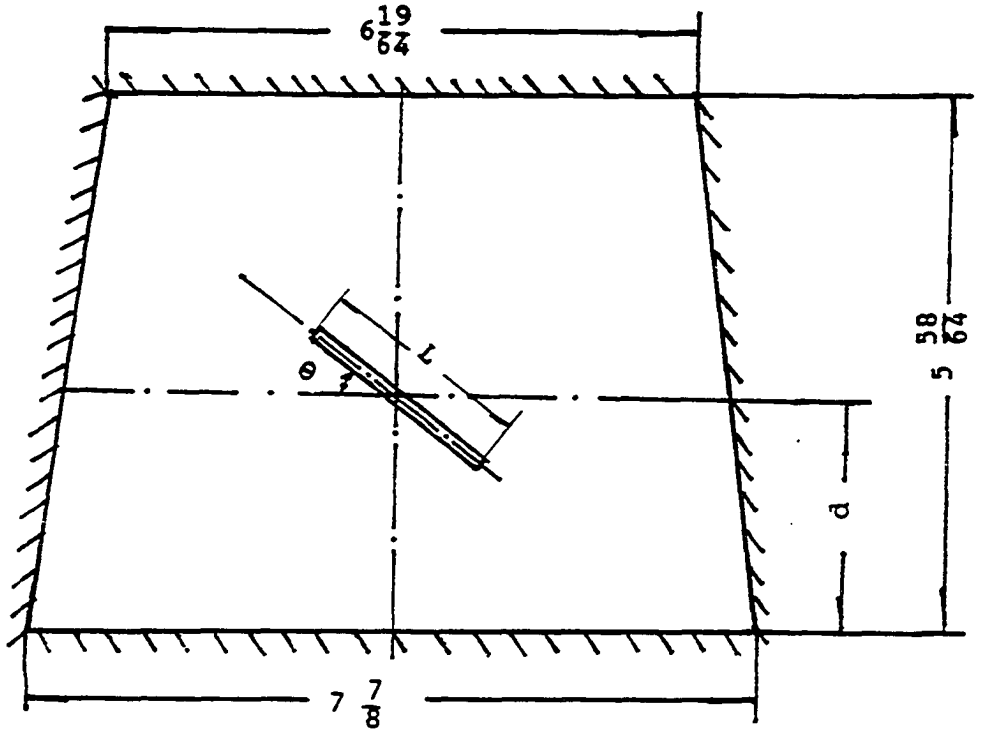

(in inch)

d = 3.0 inch for θ = 45 and 90 degrees

= 2.5 inch for θ = 0 degree

Figure 1-1. The trapezoidal plate

Both modal testing and finite element analysis were carried out as parts of the research reported here. For modal testing, an impact hammer is employed to excite plate vibration, and a near-field microphone is used to measure the response. The natural frequencies of

undamaged and damaged plates are determined from the measured frequency response function. The phase of the frequency response function is used to roughly identify the modal shapes corresponding to each natural frequency. A finite element analysis is included to corroborate modal testing results and to facilitate parameter studies. The finite element analysis uses a three node triangular element. Natural frequencies and modal shapes are calculated using the ADINA finite element package.

In the following chapter, the basic concepts of modal testing and common methods used in modal parameter estimation are introduced. Chapter III contains a description of the experimental procedures followed by a presentation and discussion of the measured results. In Chapter IV, the finite element model is described and numerical results are presented. The effects of slot width, length, and orientation are also discussed in Chapter IV. The dissertation concludes with a summary of the results and recommendations for further research.

II. MODAL TESTING

Modal testing is an experimental approach in which the dynamic behavior of an elastic structure is characterized by its modes of vibration. Each mode has parameters associated with it that may be identified from measurements at any point on the structure. Furthermore, there is a characteristic "modal shape" that defines the mode spatially over the entire structure.

The main function of modal testing is to extract the modal parameters from analysis of the measured frequency response function (FRF). The general scheme for measuring the FRF consists of measuring simultaneously the input and response signals, transforming these signals to the frequency domain, and estimating the FRF by dividing the transformed response by the transformed input. The development, within the last decade, of both digital hardware and computer algorithms for various transforms has made digital signal processing a practical method for the implementation of modal analysis for structural dynamics problems.

Although the name is relative new, the principles of modal testing were laid down many years ago. These have evolved through various phases from a time when descriptions such as 'Resonance Testing' and 'Mechanical Impedence Methods' were used to describe the general area of activity. One of the more important milestones in the development of the subject was provided by Kennedy and Pancu in 1947 [11]. The methods described found application in the accurate determination of

natural frequencies and damping factors in aircraft structures and were not out-dated for many years, until the rapid advance of measurement and analysis techniques in the 1960s. In 1963, Bishop and Gladwell [12] described the state of resonance testing theory which, at that time, was considerably in advance of its practical implementation. By 1970, there had been major advances in transducers and electronics, digital signal analyzers had been developed and current techniques of modal testing had been established. There are a great many papers that relate to this period, and a bibliography of several hundred such references now exists [13], [14]. Among them, there are several works that should be mentioned. Richardson and Potter [15] developed a technique that is based upon digital signal processing and the fast Fourier transform to obtain frequency response function estimates. They used a least squared error estimator to identify modal properties from the measured frequency response data. Halvorsen and Brown [16] discussed the application of impulse excitation techniques and reviewed special problems encountered in practice and the techniques that have been developed for dealing with those problems. Ramsey [17] introduced the so called 'Band Selectable Fourier Analysis' or *zooming* technique for modal testing. Ewins summarizes the development of modal testing techniques in the last decade in his book [18].

In this chapter, the FRF which is the basis for modal testing techniques will be developed. Several methods for estimating modal parameters will be described, and experimental techniques used in the research will be discussed.

A. Modal Testing

The theoretical foundations of modal testing are of paramount importance to its successful implementation. Thus, it is appropriate to first deal with the basic concepts that are used at different stages of modal testing. The single degree of freedom system will be used to present these basic concepts. It should be pointed out that although very few practical structures can realistically be modelled as single degree of freedom systems, the concepts and analysis procedures of single degree of freedom systems are very useful for averaged modal testing situations [19]. For structures with modes that are well separated, single degree of freedom techniques result in very accurate answers. For structures with high modal density, the single degree of freedom techniques often give good results if exciter positions are chosen to minimize modal interaction. These two situations encompass the majority of test structures encountered.

1. Single degree of freedom system theory

Fig. (2-1) shows a single of freedom system(SDOFS) with mass m, spring stiffness k, damping c, and exciting force f(t). The steady state response of the system to an exciting force $f(t) = fe^{i\omega t}$ can be assumed to be of the form

$$x(t) = X\, e^{i\omega t}$$

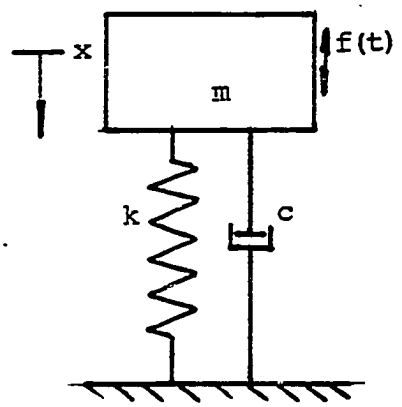

Figure 2-1. Single degree of freedom model

The equation of motion is

$$(-\omega^2 m + i\omega c + k)\, x\, e^{i\omega t} = f\, e^{i\omega t}$$

The FRF is defined as

$$H(\omega) = x/f = 1/(-\omega^2 m + k + i\omega c) \qquad (2\text{-}1)$$

which is complex, containing both magnitude and phase information. Note that the FRF magnitude is

$$|H(\omega)| = 1/\sqrt{(k - \omega^2 m)^2 + (\omega c)^2} \qquad (2\text{-}2)$$

and the phase is

$$H(\omega) = \angle x - \angle f = \tan^{-1}\left(-\omega c / (k-\omega^2 m)\right) \qquad (2\text{-}3)$$

Equation (2-3) indicates that the phase of the FRF is the angle between the exciting force and the response. Fig. (2-2) illustrates a geometrical interpretation of the phase information of the FRF for a single degree of freedom system.

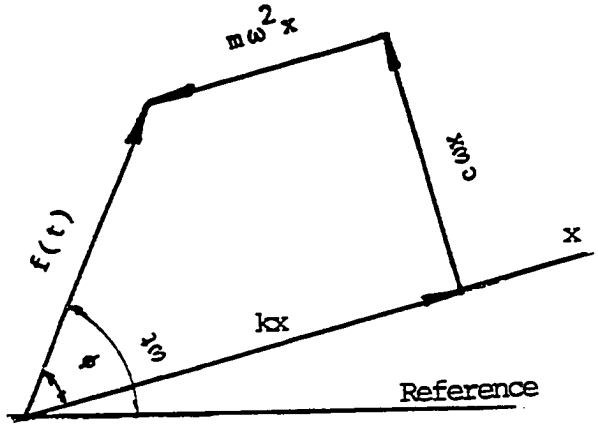

Figure 2-2. Single degree of freedom response phase angle

The FRF can also be written in complex notation with real and imaginary parts as

$$H(\omega) = \frac{k-\omega^2 m}{(k-\omega^2 m)^2 + (\omega c)^2} - i\frac{c\omega}{(k-\omega^2 m)^2 + (\omega c)^2} \qquad (2\text{-}4)$$

There are three common ways in which the FRF is displayed. The most popular display is the Bode plot consisting of two graphs. One graph is a plot of the magnitude of the FRF vs frequency, while the other one is a plot of its phase vs frequency. A second display is the Nyquist plot. In a Nyquist plot, the FRF is displayed as a plot of real part vs imaginary part. No frequency information is contained explicitly in a Nyquist plot. In general, the Nyquist plot of a SDOFS approaches a circle near the natural frequency. This can be shown as follows.

Let R be the real part of FRF, from Eq. (2-4)

$$R = \frac{k - \omega^2 m}{(k-\omega^2 m)^2 + (c\omega)^2} \tag{2-5}$$

and the imaginary part I is

$$I = \frac{c\omega}{(k -\omega^2 m)^2 + (c\omega)^2} \tag{2-6}$$

Let $L = I - 1/(2\omega c)$ and the following relation can be found

$$R^2 + L^2 = (1/2\omega c)^2 \tag{2-7}$$

As ω approaches ω_0 Eq. (2-7) becomes

$$R^2 + L^2 = (1/2\omega_0 c)^2 \tag{2-8}$$

which is the equation of circle.

For structural damping that is inversely proportional to frequency

$$c = b/\omega \qquad (2\text{-}9)$$

and substituting Eq. (2-9) to Eq. (2-7), gives

$$R^2 + L^2 = (1/2b)^2$$

which is exactly a circle.

A third form of display for the FRF also contains two graphs which are plots of the real part of FRF vs frequency and the imaginary part vs frequency.

2. Multi-degree of freedom system (MDOF) and modal shape

For an undamped N degree of freedom system, the governing equation of motion can be written in matrix form as

$$[M] \{x\} + [K] \{x\} = \{f\} \qquad (2\text{-}10)$$

where, [M] is a NxN mass matrix

[K] is a NxN stiffness matrix

$\{x\}$ is a Nx1 displacement vector

$\{f\}$ is a Nx1 force vector.

The natural frequencies and modal shapes can be determined from the solution of the free vibration equation by taking

$$\{f\} = \{0\}$$

In this case, the solution can be assumed to be of the form

$$\{x\} = \{D\}\, e^{i\omega t} \tag{2-11}$$

where {D} is a Nx1 vector of time-independent amplitudes.
It is clear that

$$\{\ddot{x}\} = -\omega^2 \{D\} e^{i\omega t} \tag{2-12}$$

Substitution of Eqs. (2-11) and (2-12) into the free vibration equation of motion, leads to

$$([K] - \omega^2 [M])\{D\}\, e^{i\omega t} = \{0\} \tag{2-13}$$

for which the only non-trivial solution must satisfy

$$\det |[K] - \omega^2 [M]| = 0 \tag{2-14}$$

The above condition is an equation of order N in ω^2. The N undamped natural frequencies of the system are the solutions of Eq. (2-14).

Substituting any one of these N values of the natural frequency back into Eq. (2-14) yields a corresponding set of relative values of {D}, the so called modal shape or eigenvector $\{\psi\}$, corresponding to that natural frequency. The complete solutions for the natural frequencies and modal shapes can be expressed in two NxN matrices, the

eigenmatrices, as

$$\begin{bmatrix} \omega_1^2 & & & \\ & \omega_2^2 & & \\ & & \ddots & \\ & & & \end{bmatrix}$$

and

$$[\psi]$$

where ω_i^2 is the ith eigenvalue, or squared natural frequency, and $[\psi]$ is a description of the corresponding modal shape.

The FRF of MDOFS can be derived from the forced vibration equation, Eq. (2-10). We consider the case in which the structure is excited sinusoidally by a set of forces of the same frequency, ω, but with different amplitudes and phases. That is

$$\{f\} = \{F\} e^{i\omega t} \tag{2-15}$$

The solution of Eq. (2-10) is again assumed to be of the form

$$\{X\} = \{D\} e^{i\omega t} \tag{2-16}$$

where $\{F\}$ and $\{D\}$ are Nx1 vectors of time-independent complex amplitudes. Substituting Eqs. (2-15) and (2-16) into Eq. (2-10), the equation of motion becomes

$$([K] - \omega^2 [M])\{D\} e^{i\omega t} = \{F\} e^{i\omega t} \qquad (2\text{-}17)$$

Thus, the response can be written as

$$\{D\} = \left[[K] - \omega^2 [M] \right]^{-1} \{F\}$$

or

$$\{D\} = [H(\omega)] \{F\}$$

where $[H(\omega)]$ is the NxN frequency response matrix for the MDOFS. It can be expressed as

$$[H(\omega)] = ([K] - \omega^2[M])^{-1} \qquad (2\text{-}18)$$

The general element in the frequency response matrix, $H_{jk}(\omega)$, is defined as

$$H_{jk}(\omega) = \left(\frac{X_j}{F_k}\right) \qquad (2\text{-}19)$$

which is similar to the definition for the SDOF system, where X_j is the response at the jth point for excitation F_k acting at the kth point.

The frequency response matrix can also be derived using the orthogonal property of the modal shapes. Equation (2-18) can be written as

$$([K] - \omega^2[M]) = [H(\omega)]^{-1} \qquad (2\text{-}20)$$

Pre- and post-multiply both sides of Eq. (2-20) by $[\phi]^T$ and $[\phi]$, where $[\phi]$ is the normalized modal shape matrix, and noting that

$$[\phi]^T [M] [\phi] = \begin{bmatrix} I \end{bmatrix}$$

$$[\phi]^T [K] [\phi] = \begin{bmatrix} \omega_r \end{bmatrix}$$

gives

$$[H(\omega)] = [\phi] \left[(\omega^2_r - \omega^2) \right]^{-1} [\phi]^T \qquad (2\text{-}21)$$

It is clear from this expression that the frequency response matrix is symmetric. That is

$$H_{jk} = (X_j/F_k) = H_{kj} = (X_k/F_j)$$

Any element of the frequency response matrix can be computed from Eq. (2-21) using the formulae

$$H_{jk}(\omega) = \sum_{r=1}^{N} \frac{{}_r\phi_j \; {}_r\phi_k}{\omega^2_r - \omega^2} \qquad (2\text{-}22)$$

or

$$H_{jk}(\omega) = \sum_{r=1}^{N} \frac{{}_rA_{jk}}{\omega_r^2 - \omega^2}$$

which is a simpler and more informative expression than Eq. (2-18). In Eq. (2-22), ${}_rA_{jk}$ is a new parameter which is referred to as a modal constant (note that the modal constant is also called the 'residue' in some papers).

Equation (2-22) is an important result for modal testing. It is in fact the central relationship upon which the method is based. In modal testing, the frequency response values at a certain point j can be measured. The natural frequency ω_r can be estimated from the measured FRF. Hence, Eq. (2-22) can be used to estimate the modal constant or the modal shape.

So far the FRF, $H(\omega)$, has been defined as the ratio of a harmonic displacement response to the harmonic excitation force. This quantity is usually called the receptance FRF. There are two alternative ways to define FRF, the mobility FRF, and the inertance FRF. The mobility FRF, $Y(\omega)$, is defined as the ratio of a harmonic velocity response and the harmonic excitation force, while the intertance formulation uses acceleration as the response parameter.

The frequency response function contains all the information that is necessary to characterize the dynamic system. Unfortunately, the measured frequency response function is presented as a set of discrete values rather than in mathematical form. There is a gap between the

measured and theoretical expressions of the FRF. The techniques that extract the natural frequency, damping factor, and modal shape from a measured FRF bridge the gap, and are referred to as parameter estimation. This topic will be discussed in more detail in the next section.

B. Parameter Estimation

Experimental modal analysis has become an increasingly popular technique in recent years. Developments in measurement and instrumentation technology have facilitated the acquisition of data of sufficient accuracy for the extraction of the modal properties of a structure under test.

One of the earliest such techniques to be applied to mechanical structures is a graphical analysis method developed by Salter [20]. The graphical method is based upon the fact that frequencies of resonance and antiresonance are determined by the mass and stiffness of a structure. The recent development of numerical modal analysis algorithms has been extensive, and the curve fitting procedures upon which they are based are very refined.

The purpose of parameter estimation is to identify the modal parameters including the natural frequency, damping coefficients, and modal shapes from measured structural response. The modal parameters of a structure are of prime interest, since these parameters define the dynamical behavior of the structure in a very concise mathematical manner. The present section describes some of the procedures used in

this work.

In order to evaluate the success or failure of the modal estimation method, the original data are often compared to a curve that has been generated from the estimated modal parameters. This comparison of curves, referred to as curve-fitting, is one measure of the validity of modal parameter estimation. A variety of software [15],[21] has been developed for this purpose. The algorithm used in particular software may be different, but the basic concepts are the same. The description given here will focus on the basic concept.

In most modal parameter estimation schemes, the typical procedure is to estimate the natural frequency and damping factor using either the magnitude of the frequency response function or the imaginary part of the response. After the natural frequency has been determined, the modal constant or modal shape can be estimated using Eq. (2-22).

1. Amplitude response

Perhaps the simplest modal parameter estimation procedure is to measure the magnitude of the FRF at one of the natural frequencies. The natural frequencies can be determined since they are the frequencies of maximum response. The damping factor can be determined using a half-power point method [22]. After determining the natural frequencies and damping factors, the modal constant can be found from the equation

$$A_r = |H_r| \omega^2_r \xi_r$$

where, H_r is the measured FRF value at the rth natural frequency, ω_r^2 is the estimated rth natural frequency, and ξ is the estimated damping factor [18]. An advantage of this method is that a minimum amount of equipment is used.

2. Quadrature(imaginary) response

The quadrature or imaginary part of the frequency response function of the tested system reaches a maximum at the undamped natural frequency and approaches zero away from the natural frequency. This property can easily be shown from Eq. (2-16). The influence of damping on the natural frequency is thus eliminated making it easier to separate the adjacent modes. For cases where the system is lightly damped or the modes are well-separated, the quadrature response is a very good method.

So far, systems have been discussed in terms of a single degree of freedom model that can be used for exactly single degree of freedom systems as well as for multi-degree of freedom systems that have well spaced natural frequencies. In MDOF systems neighboring modes are observed to contribute a noticeable amount to the total response, even when adjacent modes are well separated. In order to deal with this kind of problem, a more general type of curve-fit method, called a multi-degree of freedom system (MDOFS) curve-fit procedure will be discussed next.

3. Lightly damped MDOFS

In this section, a class of structures that may be modelled as undamped MDOFS will be considered. The class includes structures in which the damping is both relatively small and of no intrinsic interest. This situation is encountered in a great many practical applications, and especially those involving investigations of individual components that form part of an assembled structure. Usually, the individual components are themselves very lightly damped, and the damping they possess is often of little consequence to the assembled structure. The modal parameter estimation method for this kind of structure is described below.

For an effectively undamped system, the FRF can be expressed by Eq. (2-22) as

$$H_{jk}(\omega) = \sum_{r=1}^{N} \frac{{}_rA_{jk}}{\omega^2_r - \omega^2}$$

which, for a specific value measured at frequency, Ω_1, can be rewritten in the form

$$H_{jk}(\Omega_1) = \{(\omega_1^2 - \Omega_1^2)^{-1}(\omega_1^2 - {}_2\Omega_1)^{-1} \ldots .\} \begin{Bmatrix} {}_1A_{jk} \\ {}_2A_{jk} \\ \vdots \\ \vdots \end{Bmatrix}$$

If m such individual measurements are made, these equations can be expressed in the form

$$\begin{Bmatrix} H_{jk}(\Omega_1) \\ H_{jk}(\Omega_2) \\ \vdots \\ H_{jk}(\Omega_m) \end{Bmatrix} = \begin{bmatrix} (\omega_1^2-\Omega_1^2)^{-1} & (\omega_2^2-\Omega_1^2)^{-1} & \cdots \\ (\omega_1^2-\Omega_2^2)^{-1} & (\omega_2^2-\Omega_2^2)^{-1} & \cdots \\ \vdots & \vdots & \\ (\omega_1^2-\Omega_m^2)^{-1} & (\omega_2^2-\Omega_m^2)^{-1} & \cdots \end{bmatrix} \begin{Bmatrix} {}_1A_{jk} \\ {}_2A_{jk} \\ \vdots \\ {}_mA_{jk} \end{Bmatrix} \qquad (2\text{-}23)$$

or simply

$$\{H_{jk}(\Omega)\} = [R]\ \{A_{jk}\} \qquad (2\text{-}24)$$

where [R] is

$$[R] = \begin{bmatrix} (\omega_1^2-\Omega_1^2)^{-1} & (\omega_2^2-\Omega_1^2)^{-1} & \cdots \\ (\omega_1^2-\Omega_2^2)^{-1} & (\omega_2^2-\Omega_2^2)^{-1} & \cdots \\ \vdots & \vdots & \\ (\omega_1^2-\Omega_m^2)^{-1} & (\omega_2^2-\Omega_m^2)^{-1} & \cdots \end{bmatrix}$$

from which a solution for the unknown modal constants A_{jk} may be obtained in terms of the measured FRF data and the previously estimated natural frequency. That is:

$$\{A_{jk}\} = [R]^{-1} \{H_{jk}(\Omega)\} \qquad (2\text{-}25)$$

Although very simple in concept, the success of the method in practical situations depends on the points chosen for the individual FRF measurements [23]. There are two sources of error that will contaminate the result. One is that the estimated FRF is usually contaminated by random measurement errors. The other is that in most practical cases, vibration data are acquired by measurement over limited frequency ranges on a system that has many degrees of freedom and a corresponding number of modes. Thus, it is generally impossible to carry out complete modal analysis. The calculated modal constants will have errors associated with such out-of-range frequency contributions. In order to reduce this error, Ewins [18] recommends the use of as many antiresonances as are available. Methods for controlling the random errors will be discussed in the following section.

C. Experimental Considerations for the Impact Method

There are several methods used to excite a structural vibration including swept-sine, pure and pseudo random, and transient excitation. The impact method falls into the category of transient excitation. The impact method deserves particular attention because, for a wide range of structures, it is the simplest and fastest excitation method. There are, however, a number of difficulties associated with the application of the impact method. The major errors encountered in the application of the method are noise and leakage. Noise can be a problem in both the

input force and response signal measurements, and is mainly a consequence of a long analysis time compared with the impact duration. Leakage is of most concern in the response signal, and is caused by the short recording time. Another problem connected with the impact method is that the power spectrum of the input force is not as easily controlled as it is in steady-state excitation methods. This may cause non-linearities to be excited, and can result in variablity between measurements as a consequence of variations in the input force signal. A great deal of effort has been exerted by many researchers to improve impact measurement results and several special window functions have been developed to reduce the effects of noise [16]. No attempt will be made to cover all the techniques developed, but the method used in this work will be discussed.

1. Window functions

Usually, both the input force and the response signals are modified by a window function in the impact method. However, the purpose of the window function for the two signals is different. The purpose of the input force window is to reduce the noise and improve the signal to noise ratio. Typically, the force pulse has a low rms energy level even though its peak level is high. Also, the duration is short when compared with the analyzer record length. Thus, the total energy level of noise over the record length may be significant compared to the energy of the pulse. The general form of the force window is rectangular in shape which forces the signal outside the window to zero,

while the actual signal amplitude is preserved inside the window.

An exponential window is often applied to the response signal. The function of the exponential window is to force the response to be zero at the end of the record time. The measured response of the structure may not decay to zero by the end of the analyzer observation time because of the short observation time. Thus, the measurement is a truncated version of the complete response. From digital signal processing theory, a sharp truncation of the time signal will contaminate the information in the frequency domain. This contamination is called the leakage error. By forcing the response signal to zero at the end of the observation time, the leakage error is reduced.

2. Hammer

The usefulness of the impact method lies in the fact that the energy in an impact is distributed continuously in the frequency domain rather than occurring at discrete spectral lines as is the case for periodic signals. Theoretically, an impact force will excite all resonances of the test structure. Experimentally, only the resonances in a certain frequency range, the useful frequency range, will be excited. The extent of the useful frequency range is controlled by the pulse shape which is determined by the stiffness of the hammer tip and the test structure. A harder hammer tip results in a shorter pulse duration, and larger useful frequency range. Corelli and Brown [24] suggest that a good rule of thumb is to choose a tip so that the auto-power spectrum of the input force pulse is no more than 10 to 20 dB

down at the end of the frequency range of interest.

The mass of the hammer is another factor that must be considered. The mass of the hammer controls the amount energy that is transferred to the test structure. A larger mass makes more impact energy available for transfer to the structure. However, increasing the mass of the hammer also tends to increase the pulse duration. As a result, increasing the mass tends to reduce the useful frequency range.

3. Zoom

The purpose of zoom is to increase the frequency resolution and to separate strongly coupled frequencies. Narrow zoom ranges cause the analyzer observation time to become excessively long for impact testing. For example, an 800 line, 500 Hz analyzer requires a record length of 1.6 seconds. Impacting a structure once every 1.6 seconds transfers a small amount of energy into the structure, and makes modal testing a slow process. A more efficient excitation method is to use a series of randomly spaced impacts within each time record. That is, the structure is impacted several times within each observation time, thereby increasing the total energy input to the structure. When using this method, care must be taken to avoid periodic impacts or the input force spectrum will be distorted.

When using the random impact method, the transient window designed for a single impact is inappropriate since the noise problem has been solved by adding more signal. The additional energy in decibels is proportional to 10log(M) where M is the number of impacts per data

record [25]. A suitable window for both channels in random impact testing is the Hanning window. Use of a Hanning window avoids truncation of the signal at the end of the time record, and thus reduces leakage, in the frequency domain.

4. Coherence function

In practice, measurement noise is always present at both the input and the output. In this work, a microphone is used as a response transducer, and it responds to radiated sound from the plate as well as to the background noise. Thus, the measured output signal is contaminated by background noise in the laboratory. It is important to estimate the effects of noise on the measurement. The coherence function provides a means for internally estimating the quality of an experimental determination of the FRF.

The coherence function indicates whether or not the response is linearly related to the input and is defined by the equation

$$\gamma_{xy}^2(f) = \frac{G_{xy}(f)^2}{G_{xx}(f)\, G_{yy}(f)} \qquad (2\text{-}26)$$

where, $G_{xx}(f)$ is the measured input spectral density,

$G_{yy}(f)$ is the measured output spectral density,

$G_{xy}(f)$ is the cross spectral density.

Experimental contamination can be modelled by including measurement noise at both the input and output of a linear system, as shown in

Fig. 2-3.

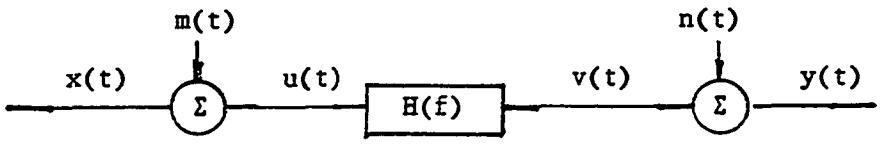

Figure 2-3. Linear system with input and output measurement noise

It follows that the measured input and output signals will be

$$x(t) = u(t) + m(t)$$

$$y(t) = v(t) + n(t)$$

where, m(t) is input measurement noise

n(t) is output measurement noise.

By assuming the noise terms to be uncorrelated with each other and with the signals, that is

$$G_{mn}(f) = G_{xm}(f) = G_{yn}(f) = 0$$

the coherence function becomes

$$\gamma_{xy}^2(f) = \frac{G_{uu}(f)\, G_{vv}(f)}{[G_{uu}(f)+G_{mm}(f)][G_{vv}(f)+G_{nn}(f)]} \qquad (2\text{-}27)$$

Equation (2-27) may be manipulated to give

$$\gamma_{xy}^{2}(f) = \left(1 - \frac{G_{nn}(f)}{G_{yy}(f)}\right)\left(1 - \frac{G_{mm}(f)}{G_{xx}(f)}\right) \qquad (2\text{-}28)$$

which explicitly shows the effects of measurement noise on the coherence function. The values of coherence function less than unity indicate that extraneous noise is present.

It should be pointed out that Eq. (2-27) is based on the assumption of linearity. If the test structure is non-linear, the coherence function will also be less than unity even though no noise is present in the measurement. Actually, the coherence is a measure of the output that is linearly related to the input.

III. EXPERIMENTAL PROCEDURES AND RESULTS

The main goal of the research described in this thesis is to investigate the relationships among changes in the natural frequencies and the dimensions and orientation of damage in a trapezoidal plate. Three identical plates with thickness of 0.0397 inch were used. Plate damage was simulated by cutting various size center slots. Slot length was varied from 2.0 to 3.0 inches for a fixed slot width of 5/64 inches. The orientation of damage in each plate is different. An impact hammer was used to excite the test plate vibration. A near field microphone was used to detect the plate response. The natural frequencies of undamaged and damaged plates were determined from measured FRFs. The phase angles of the FRFs were also measured for each case.

This chapter consists of four parts. The experimental set-up is described first. Next, the experimental procedures are discussed. The experimental results are presented in the third section and discussed in the concluding section of the chapter.

A. Experimental Set-up

1. Test plate

Figure 3-1 is a sketch of the experimental apparatus. The apparatus consists of a trapezoidal plate, two clamping frames, and eight clamping pads. The plate is made from 0.0397 inch thick aluminum, and the clamping frames and pads are made from 3/8 inch and 1/2 inch thick aluminum, respectively. In order to simulate the clamped boundary

conditions on all four sides, the test plate is clamped between two strong frames that are fastened together using 40 bolts and nuts.

The experimental apparatus is similar to that used by Maruyama in his investigation of undamaged trapezoidal plates [10]. The similar set-up was constructed so that Maruyama's results could be used to verify the experimental procedures.

2. Measurement system

The measurement system includes force and response transducers and the frequency analyzer. Figure 3-2 is a diagram of the data acquisition system. In order to obtain the frequency response function, the input force and response signals must be measured simultaneously. The input force was measured using an integral force cell that is part of the PCB impulse hammer. The input force signal from the force cell was amplified by a PCB preamplifer, and was fed to a Bruel & Kjaer Dual Channel Signal Analyzer, type 2032. The response signal was measured using a Bruel & Kjaer 1/2 inch diameter microphone. The microphone was supported by a stand that was isolated from the impact force. The distance between the microphone and the surface of the test plate was about 1/16 inch. The microphone signal was fed directly to the Bruel & Kjaer analyzer.

The advantage of using a microphone to measure the response is that no inertial mass has been added to the structure. For a light structure, such as the test plate, the inertial mass of an attached transducer could significantly influence the measured result.

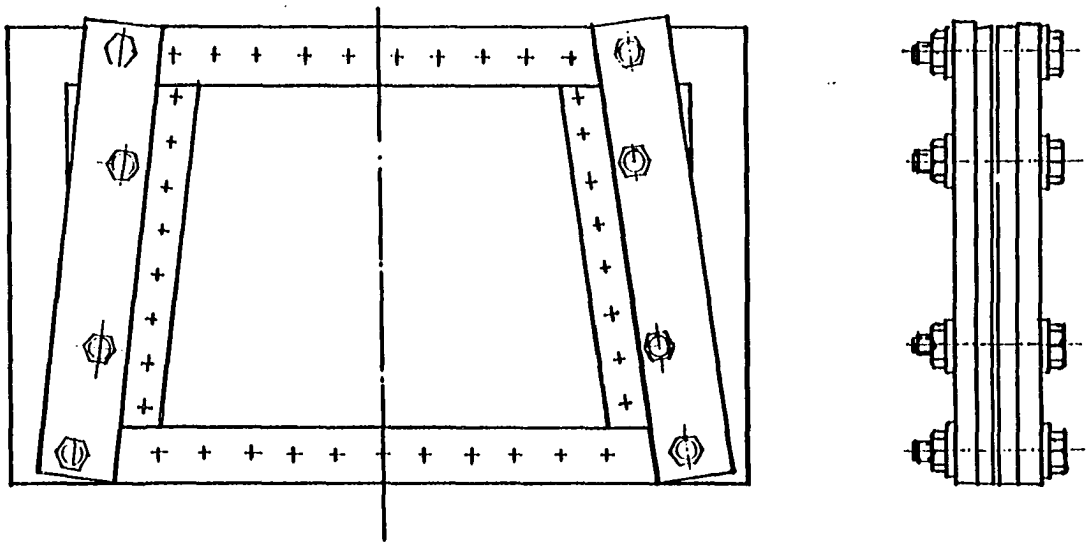

Figure 3-1. Experimental apparatus

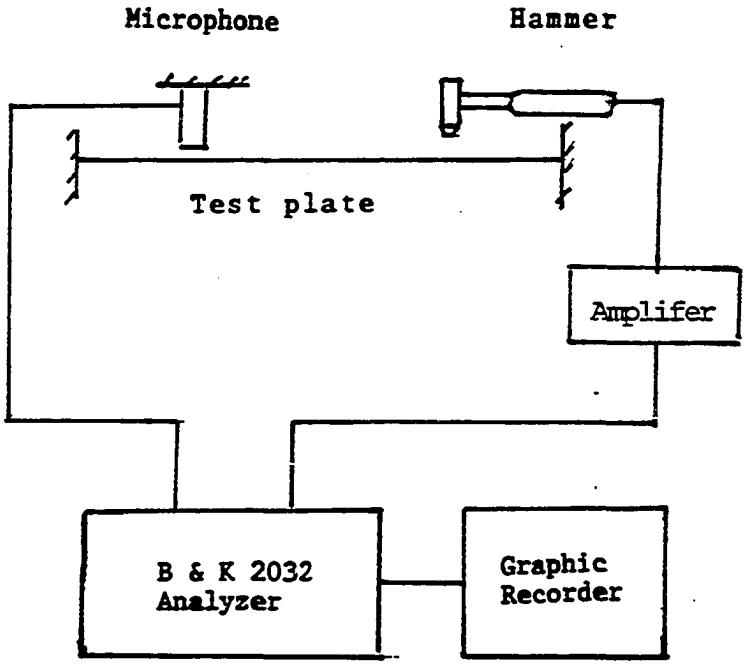

Figure 3-2. The data acquisition system

During experiments, the microphone was located very close to the vibrating surface of the plate, and it can be considered to be in the near field of the plate. The sound pressure that the microphone sensed is proportional to the vibrational velocity of the plate. Hence, the measured FRF is the mobility. Only one reference involving the use of a microphone as a response transducer for modal testing could be found. Comstock, Javidinejad, Fleming, and Collins [26] used a microphone to measure the vibrational response of a beam and a circular plate to transient loading. They compared response time histories measured by

microphone and by accelerometer. Their results showed that a microphone gave a satisfactory time history for modal analysis.

In this research, an investigation similar to that of Comstock was conducted for damaged and undamaged plates. In the investigation, a PCB 302A accelerometer was mounted on a test plate, and a microphone was positioned 1/16 inch above the accelerometer location. Each of the measured response signals was fed to a B & K analyzer. It was found that the estimated natural frequencies were very close, although the measured FRFs were not identical. Table 3-1 is a comparison of the estimated natural frequencies using different response transducers for an undamaged plate. Figure 3-3 is a plot of a typical FRF measured using a microphone, and Fig. 3-4 is a plot of typical FRF measured using an accelerometer. Both Figs. 3-3 and 3-4 are for a plate with a 3 inch slot. The results indicate that the difference between natural frequencies measured using an accelerometer or a microphone is less than 3%.

Table 3-1. Comparison of the natural frequencies measured using microphone and accelerometer

frequency(Hz)	f_1	f_2	f_3	f_4	f_5
microphone	182	282	544	720	920
accelerometer	186	288	550	734	920

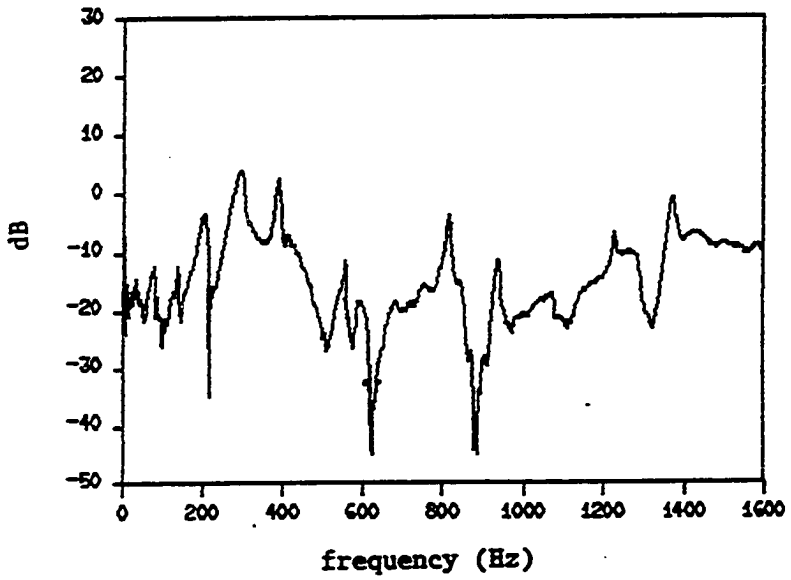

Figure 3-3. FRF measured using microphone

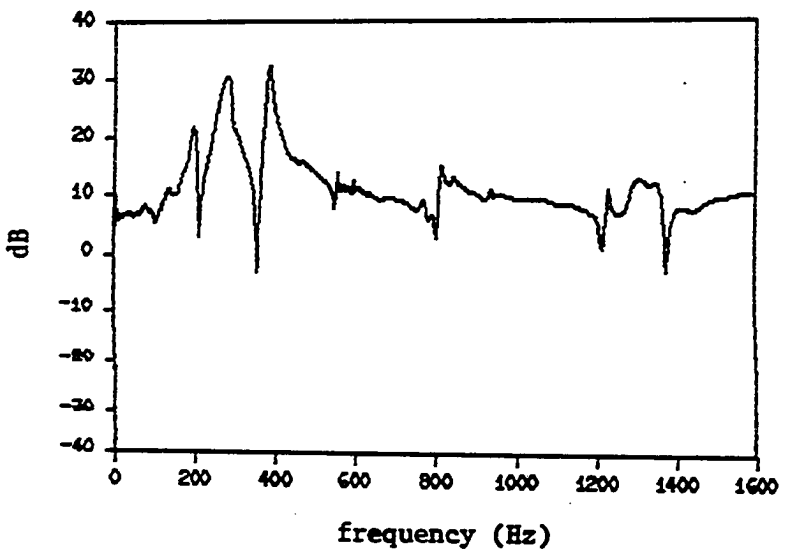

Figure 3-4. FRF measured using accelerometer

The dual channel frequency analyzer is used to record, analyze, and display the measured signals. Figure 3-5 is a listing of the measurement set-up used in the experiments. It is modified version of the standard measurement set-up No. 12 of the analyzer. The measured frequency response function can be displayed in any of the three forms discussed in the previous chapter.

MEASUREMENT SETUP

MEASUREMENT:	DUAL SPECTRUM AVERAGING
TRIGGER:	CH. A +SLOPE, LEVEL: +0.10 MAX INPUT
DELAY:	TRIG - A: -3.17 ms CH. A - B: 0.00 ms
FREQ. SPAN:	1.6 Hz ΔF: 2Hz T: 500 ms ΔT: 244 μs
CENTER FREQ:	BASEBAND
WEIGHT CH.A:	TRANSIENT SHIFT:1.95 ms LENGTH:13.18 ms
WEIGHT CH.B:	EXPON. SHIFT:1.95 ms length:199.46 ms
CH. A:	2v + 3Hz DIR FILT: 25.6 HZ 3.00 mv/N
CH. B:	2v + PREAMP FILT: 25.6 Hz 2.00 mv/m/s^2
GENERATOR:	DISABLED

Figure 3-5. The measurement set-up

B. Experimental Procedures

Three identical undamaged plates were used in the modal testing. Damage was modelled by milling 5/64 inch wide central slots in the plates at different angular orientations, as shown in Fig. 3-6. The orientations of the slots are at angles of 0, 45, and 90 degrees with respect to the base of the trapezoidal plate. The initial length of the slots is 2.0 inch. In subsequent experiments, the slot length is increased to 2.5, and finally to 3.0 inches. For each tested plate, the undamaged frequency response function was measured first. Then, for each slot length the measurement was repeated. The first five natural

frequencies and modal shapes were estimated from the measured frequency response functions for each case.

The frequency response functions were measured by impacting the plate at a fixed point, point F in Fig. 3-6, while the microphone was moved from one point to another. During the test, an ensemble of 50 excitation and response measurements was taken at each grid point and averaged. This was done to reduce noise and to ensure statistically reliable data. After each ensemble of measurements, the coherence was checked prior to proceeding with the data analysis. Fig. 3-7 shows a typical plot of the coherence for an undamaged plate.

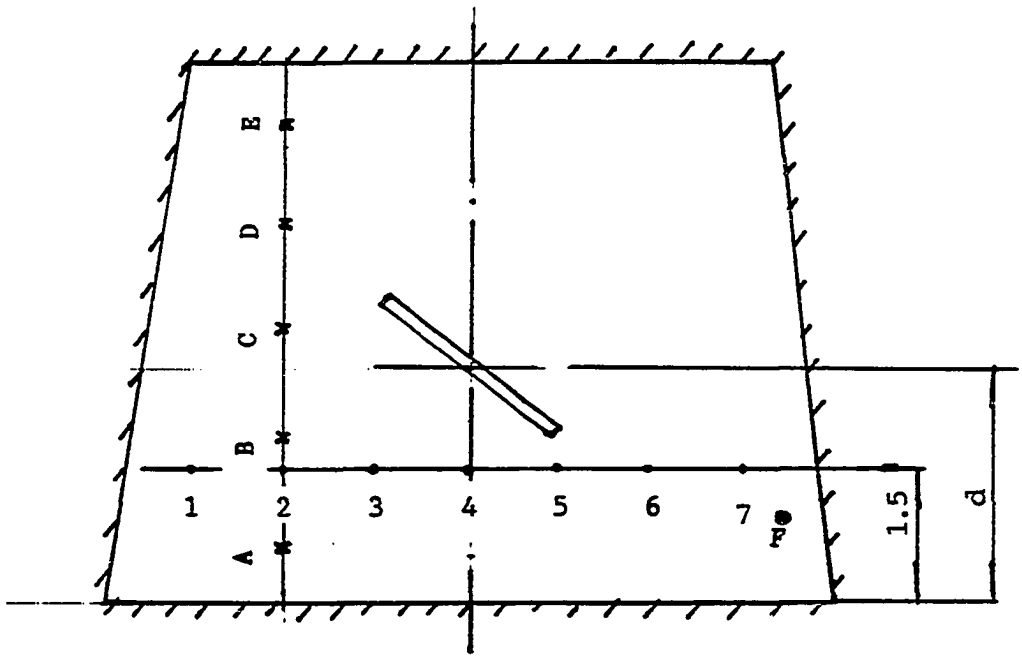

d = 3.0 in. for θ is 45 or 90 degrees
= 2.5 in. for θ is zero degree

Figure 3-6. Slot and measurement locations

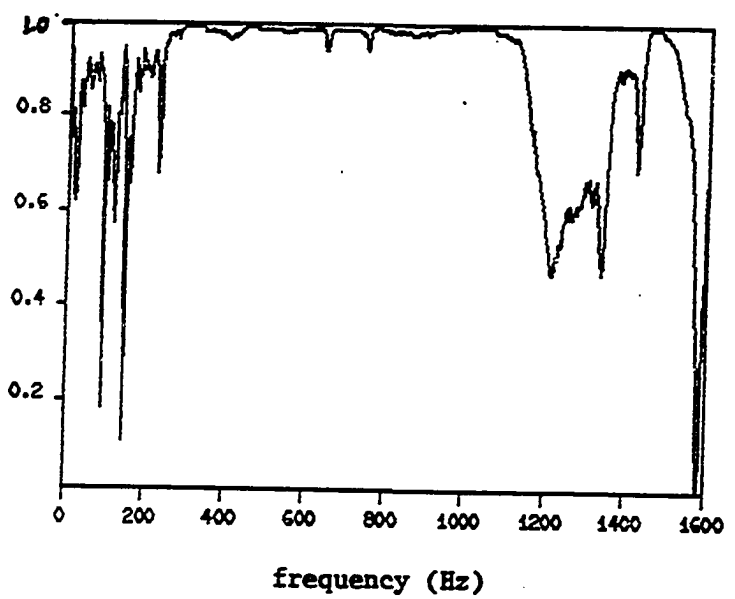

Figure 3-7. Measured coherence function for an undamaged plate

1. Estimated natural frequencies

The natural frequencies of the tested plates were determined from the measured imaginary part of the FRF. As discussed in the Chapter 2, the frequencies at which the imaginary part of the FRF reaches its maximum values are the natural frequencies. Figure 3-8 is a typical plot of the measured imaginary part of the FRF. Figure 3-9 is a plot of the real part of the FRF for the same measurement. The real part of the FRF is used to further verify the natural frequencies. Recall that Eq. (2-5) shows that at the natural frequencies the imaginary part of the FRF reaches a maximum while the real part is zero.

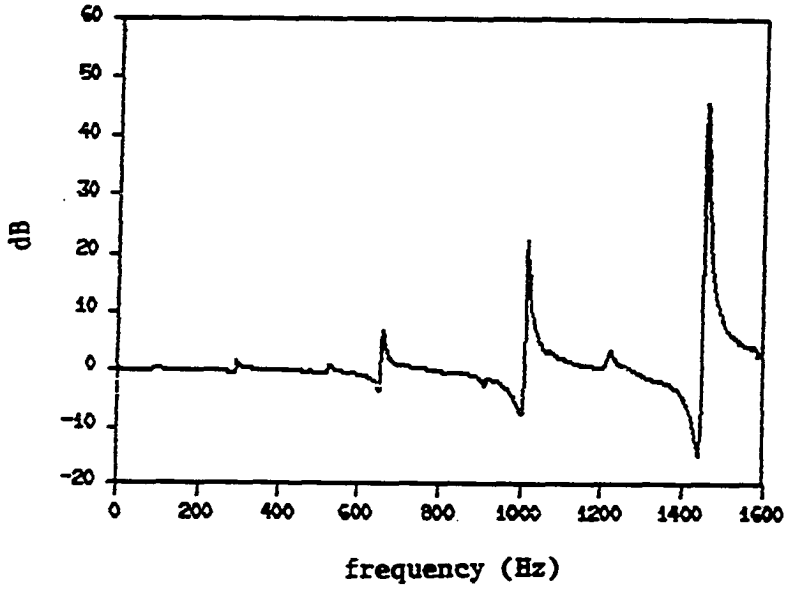

Figure 3-8. Measured imaginary part of the FRF for a plate with a 3.0 in. slot at 45 degrees

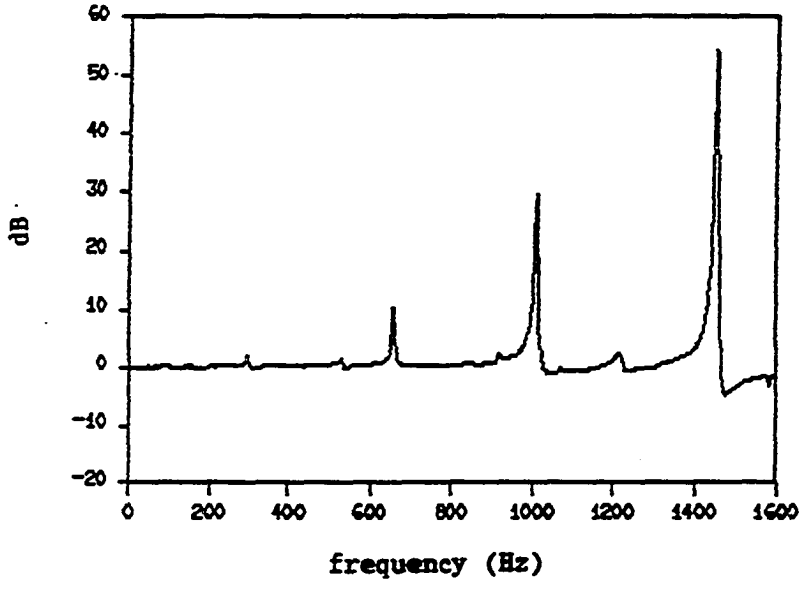

Figure 3-9. Measured real part of the FRF for a plate with a 3.0 in. slot at 45 degrees

2. Estimated modal shapes

In the course of the experimental investigation, it was found that some of the natural frequencies changed considerably, while others had little change. Because some of the natural frequencies were close together, in some instances they changed numerical order for a damaged plate. In order to accurately determine changes in natural frequencies, it is necessary to identify each frequency by verifying the corresponding modal shape. The modal shape for each natural frequency was determined roughly from the phase of the FRF. As discussed in Chapter 2, the phase of the FRF is the difference between the phase of the input force and the phase of the response. The phase difference between two points on a structure indicates the relative direction of the motion of the two positions for that particular natural frequency. The phase at each natural frequency was determined from the phase display of the FRF. Figure 3-10 is a typical phase plot. The phase of the FRF was determined for the 12 points on the plate indicated in Fig. 3-6.

C. Experimental Results

The experimental results include the natural frequencies estimated from the measured FRF and the phase information for each damage condition. In this investigation, the useful frequency range of the impact force is from 0 to 1100 Hz. For the plates investigated, this range includes the first five natural frequencies. Tables 3-2 through 3-4 contain experimentally determined estimated natural frequencies and

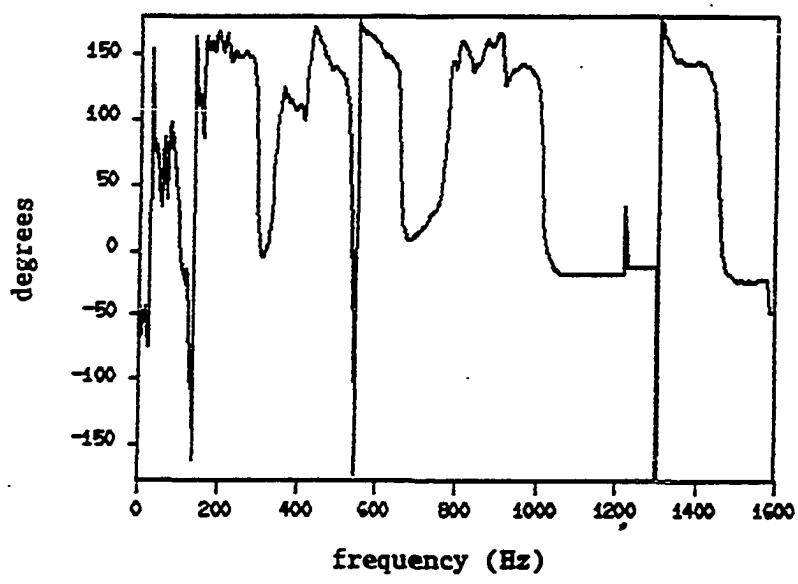

Figure 3-10. Frequency response function phase plot at measurement point No. 6 for 3.0 in. 45 degree slot

Table 3-2 contains measured natural frequencies of the plate that has a horizontal slot. Table 3-3 contains the measured natural frequencies of the plate that has a 45 degree slot. Table 3-4 contains the measured natural frequencies for the plate that has a vertical slot.

Table 3-2. Measured natural frequencies of a plate with horizontal slot (Hz)

frequency	without slot	2.0 in. slot	2.5 in. slot	3.0 in. slot
f1	344	319	318	308
f2	630	640	636	632
f3	754	707	669	605
f4	1030	1028	1020	1004
f5	1076	1090	1085	1069

Table 3-3. Measured natural frequencies of a plate with 45 degree slot (Hz)

frequency	without slot	2.0 in. slot	2.5 in. slot	3.0 in. slot
f1	332	306	304	299
f2	634	608	586	540
f3	742	720	708	694
f4	1022	962	942	916
f5	1100	1066	1060	1058

Table 3-4. Measured natural frequencies of a plate with vertical slot (Hz)

frequency	without slot	2.0 in. slot	2.5 in. slot	3.0 in. slot
f1	330	324	316	309
f2	628	598	574	521
f3	750	750	736	728
f4	1020	1020	1020	976
f5	1090	960	947	928

Tables 3-5 and 3-6 contain the measured phases for the plate that has a vertical slot.

Table 3-5. Measured FRF phases for an undamaged plate (in degrees)

Points	f1	f2	f3	f4	f5
1	99.3	-97.2	97.3	-114.1	72.6
2	98.2	-92.3	93.1	-110.5	84.3
3	96.9	-97.2	81.8	-114.5	-81.6
4	96.0	0	75.8	0	-86.1
5	99.2	84.3	63.5	65.7	-63.6
6	101.2	85.9	65.2	71.0	75.8
7	90.9	87.0	79.3	77.2	71.3
A	101.8	-104.9	87.6	-105.7	70.1
B	92.5	- 92.9	98.8	-118.5	77.6
C	91.2	- 87.1	0	0	83.0
D	82.1	-107.2	-129.7	78.7	66.2
E	79.4	- 97.7	-110.2	75.9	0

Table 3-6. Measured FRF phases for a plate with a 3.0 in. vertical slot (in degrees)

Points	f1	f2	f3	f4	f5
1	84.7	-109.0	89.2	55.9	-92.7
2	73.8	-112.3	94.7	50.4	-85.6
3	70.7	- 99.9	93.6	-48.6	-87.7
4	73.5	- 94.9	91.2	-60.3	-80.6
5	71.3	84.4	88.9	-45.2	79.6
6	77.3	86.1	94.7	74.9	79.7
7	80.8	88.0	84.2	79.8	76.9
A	84.9	- 93.9	83.5	48.5	-94.7
B	85.8	- 97.7	97.4	67.9	-85.7
C	70.8	- 96.2	81.3	72.3	-79.7
D	74.7	-117.0	-85.4	78.0	91.8
E	87.6	-107.0	-81.3	81.0	101.7

D. Discussion

Careful examination of the measured data reveals a number of interesting features.

1. The variation of the natural frequencies of undamaged plates

Three identical trapezoidal plates were used in the experiment. Theoretically, the natural frequencies should be the same for all three plates. However, the measured results show that the first five frequencies vary from one plate to another. Table 3-7 is a compilation of the measured natural frequencies from Tables 3-2 through 3-4 for the three undamaged plates. The last column shows the standard deviation as a percentage of the measured natural frequencies with respect to the mean. It shows that the lowest frequency has the largest deviation.

Table 3-7. Comparison of measured natural frequencies for three undamaged plates (Hz)

frequency	No. 1	No. 2	No. 3	Mean	Deviation (%)
f1	344	332	330	335	2
f2	630	634	628	631	0.5
f3	754	742	750	749	1
f4	1030	1022	1020	1024	1
f5	1076	1100	1090	1089	1

There are several potential reasons for the deviation, including differences in the dimensions of the plates and measurement errors. The most significant reason is probably the tension caused by mounting the plate in the frame. Since the test plates are very thin, the assembling tension may cause changes in the natural frequencies. In order to reduce the effect of the assembling stress on the natural frequency, the measurements of undamaged and damaged plates were made under the same mounting conditions. That is, after the test plate was fixed in the frame, the natural frequencies for the undamaged plate were measured. Then, the slot was cut without dismounting the plate, and the frequencies for the slotted plate were measured. Thus, the influence of the mounting condition on the natural frequencies was minimized. The results that are contained in Table 3-7 suggest that the natural frequencies of the plate can be measured with a repeatability within 1 to 2 percent.

2. Changes in the natural frequencies of the plate with a horizontal slot

Table 3-8 summarizes the changes in measured natural frequencies for a plate with different length horizontal slots. The changes were calculated from data presented in Table 3-2. The relative changes, expressed as a percentage of the undamaged natural frequencies, are also listed. The results show that frequency f3 exhibits the largest relative change. Frequency f1 also changes considerably, but the frequencies f2, f4, and f5 show no significant change. The data also indicate that f3 decreases rapidly with increasing slot length. Unexpected increases in natural frequencies f2 and f5 may be caused by the partial release of the assembling stress when a slot is cut, or by the measurement errors in the determination of natural frequency.

Table 3-8. Changes in the natural frequencies of a plate with a horizontal slot

	without slot	2.0" slot	in %	2.5" slot	in %	3.0" slot	in %
Δf1	0	-25	-7	-26	-8	-36	-10
Δf2	0	10	2	6	1	2	< 1
Δf3	0	-47	-6	-85	-11	-149	-20
Δf4	0	-2	0	-10	-1	-26	- 3
Δf5	0	14	1	9	1	-7	- 1

3. Changes in the natural frequencies of the plate with a 45 degree slot

Table 3-9 summarizes the changes and relative changes in natural frequencies of a plate with different length 45 degree slots. The changes were calculated from data presented in Table 3-3. The data show that all five frequencies exhibit considerable change for this case. For the 2.0 and 2.5 inch slots, f1 has the largest change. The second frequency, f2, also has a large change. The changes in the other frequencies are also significant. As slot length increases, the second natural frequency decreases rapidly, and for a 3.0 inch slot, f2 has the largest change.

Table 3-9. Changes in the natural frequencies of a plate with a 45 degree slot

	without slot	2.0" slot	in %	2.5" slot	in %	3.0" slot	in %
Δf1	0	-26	-8	-29	-9	-33	-10
Δf2	0	-26	-4	-48	-7	-92	-15
Δf3	0	-22	-3	-36	-5	-47	- 6
Δf4	0	-60	-6	-80	-8	-105	-10
Δf5	0	-44	-4	-50	-5	-55	-5

4. Changes in the natural frequencies for the plate with a vertical slots

Table 3-10 summarizes the changes and relative changes in measured natural frequencies of a plate with different length vertical slots. The changes were calculated from data presented in Table 3-4. The data

show that the second and fifth frequencies exhibit the largest changes. The first frequency also has considerable change, but frequencies three and four show little change. The data also show that the second frequency decreases more rapidly than fifth.

Table 3-10. Changes in the natural frequencies of a plate with a vertical slot

	without slot	2.0" slot	in %	2.5" slot	in %	3.0" slot	in %
Δf1	0	-6	- 2	-14	- 4	-21	- 6
Δf2	0	-30	- 5	-52	- 8	- 107	-17
Δf3	0	0	0	-14	- 2	-22	- 3
Δf4	0	0	0	0	0	-44	- 4
Δf5	0	-130	- 11	-143	-13	-162	-15

5. Association of natural frequency and modal shape

The modal shape corresponding to a natural frequency can be determined roughly from the measured phase information. For example, the modal shape of f4 for an undamaged plate can be estimated as follows. From Table 3-5, the measured phase indicates that points 1 through 3 are moving out of phase with points 5 through 7, while points A and B are moving out of phase with points D and E. By using the symmetry of the structure, the modal shape of f4 can be estimated as sketched in Fig. 3-11, which is consistent with the modal shape given by Maruyama et al. [10].

This method is useful for finding the change in natural frequency.

By carefully comparing the last two columns of Tables 3-5 and 3-6, it will be found that the modal shape of f4 for a 3.0" slot is similar to the modal shape of f5 for a plate with no slot. Thus, the fourth natural frequency of the plate with a 3.0 inch slot corresponds to the fifth natural frequency of the same plate without a slot. When calculating changes in natural frequency, it is important to associate natural frequencies with modal shape rather than numerical order.

The experimental results indicate that the presence of a slot influences the natural frequencies of a plate in a measurable way. The results also suggest that the length and orientation of the slot have a significant effect on changes in natural frequency. The results presented in this chapter will be compared with numerical predictions obtained using a finite element model and discussed more extensively in the following chapter.

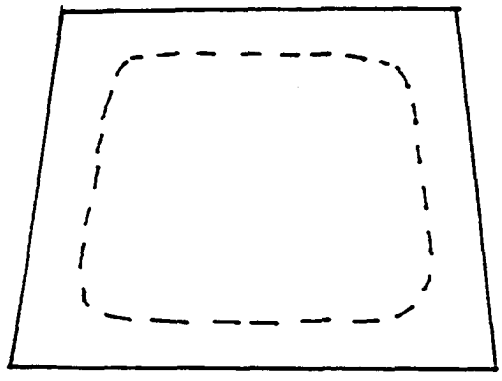

332 (Hz)

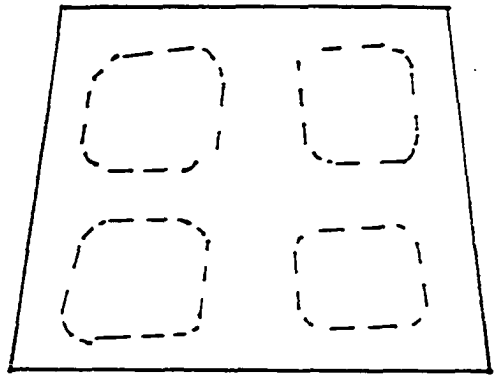

1030 (Hz)

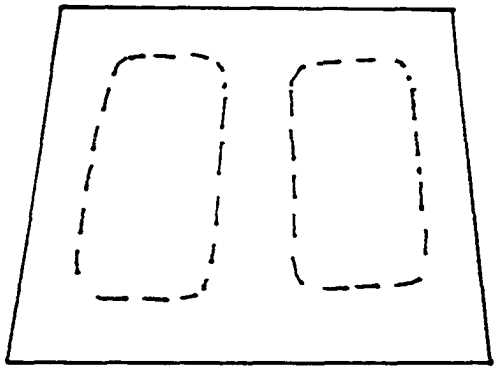

617 (Hz)

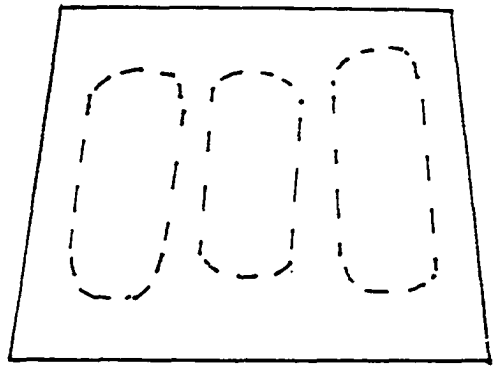

1076 (Hz)

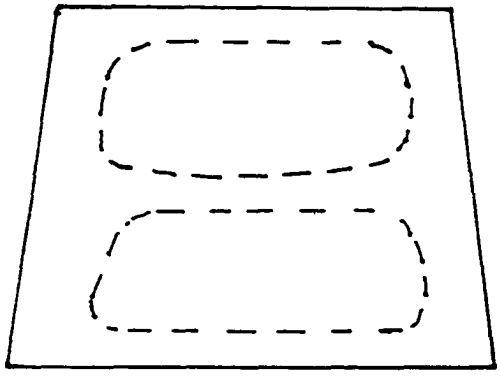

742 (Hz)

Figure 3-11. Estimated modal shape for an undamaged plate

IV. FINITE ELEMENT MODEL

A. Introduction

The natural frequencies and modal shapes of the tested plates can be predicted using the finite element method. The governing differential equation of motion for transverse vibrations of a thin isotropic plate is

$$D\nabla^4 w + \rho h \partial^2 w/\partial t^2 = 0 \qquad (4\text{-}1)$$

where D is the flexural rigidity, defined by

$$D = Eh^3/12(1-\nu^2)$$

E is the Young's modulus, ν is Poisson's ratio, ρ is the mass density, and h is the thickness of the plate (for further discussion of Eq. 4-1 see, for example, ref. 27).

Equation (4-1) cannot be solved analytically for the natural frequencies and modal shapes for most boundary conditions. Thus, the finite element method is often used to estimate the natural frequencies and modal shapes. The usual finite element strategy is to determine the frequency and modal shape from the eigenvalue equation

$$\det ([K] - \omega^2[M]) = 0 \qquad (4\text{-}2)$$

The stiffness matrix [K] is obtained from the strain energy expression

$$\frac{1}{2}\int_0^a\int_0^b \left[\left(D\frac{\partial^2 w}{\partial x^2}\right)^2 + D\left(\frac{\partial^2 w}{\partial y^2}\right)^2 + 4D_{33}\left(\frac{\partial^2 w}{\partial x \partial y}\right)^2 + 2D_{12}\left(\frac{\partial^2 w}{\partial x^2}\frac{\partial^2 w}{\partial y^2}\right)\right] dxdy$$

where $D_{33} = D\ (1 - \nu)/2$, $D_{12} = D\nu$

and the mass matrix [M] is obtained from the kinetic energy expression

$$\frac{1}{2}\int_0^a\int_0^b \rho h\left(\frac{\partial w}{\partial t}\right)^2 dxdy$$

Finite element analysis is used in connection with this research for two reasons. One is to obtain independent estimates for the natural frequencies and modal shapes to compare with the experimental results. A numerical corroboration of the experimental results is desirable because there are a number of potential measurement errors. A second reason for using the finite element method is to facilitate parameter studies. In the experimental work, the slot width used is 5/64 inch, the smallest milling cut that can be made in the ERI workshop. In order to study the influence of a narrower slot on the natural frequency, a finite element analysis was carried out. There is no limitation on the slot width for a finite element model. The finite element model is more flexible than the experimental method, and it is also more efficient and convenient for parameter studies.

In this research, the ADINA [28] package of finite element software was used to extract the natural frequencies and modal shapes for a

trapezoidal plate. The finite element model for an undamaged plate consisted of 335 3-node thin plate triangular elements spanning 195 nodes. The total number of degrees of freedom for this model was 525. Figures 4-1 and 4-2 show the meshes for typical undamaged and damaged plates.

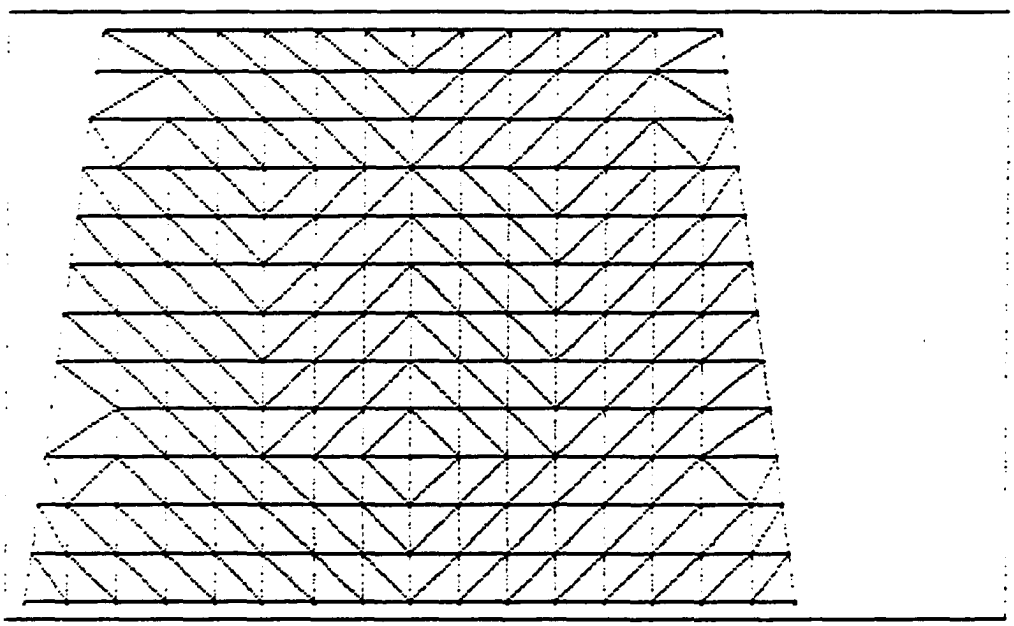

Figure 4-1. Finite element mesh for an undamaged plate

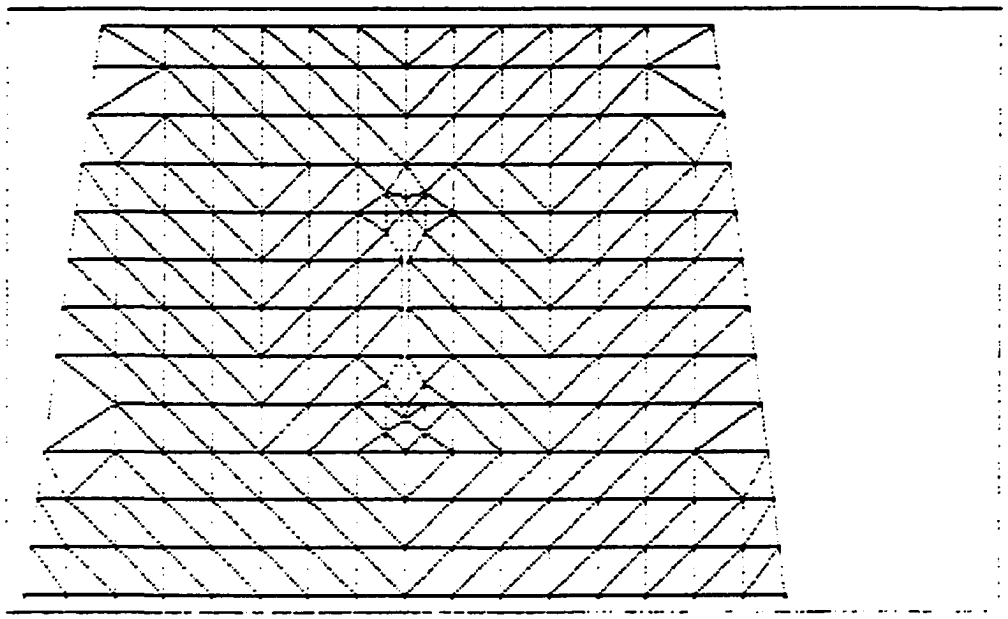

Figure 4-2. Finite element mesh for a plate with a 2.0 in. by 5/64 in. vertical slot

The finite element analysis that was conducted in connection with this research can be divided into three phases. Phase 1 was a test of the finite element model by comparison of the finite element results with numerical and experimental results given by Maruyama et al. [10]. Phase 2 consisted of a comparison between finite element and experimental results obtained as part of this research. Finally, phase 3 was a parameter study of the effect of slot width on natural frequency. The parameter study consisted of numerical estimates of

frequencies and modal shapes for four different slot widths. The results for each phase will be presented in the next section. The effects of the length, orientation, and width of the slot on natural frequencies will also be discussed.

B. Finite Element Results and Discussion

The finite element analysis was carried out on a NAS/9 main frame computer using the ADINA finite element package. Only the natural frequencies and modal shapes were calculated.

1. Comparison of finite element results with Maruyama's results

The finite element model was tested by comparing the finite element results with the numerical results given by Maruyama for an undamaged plate. In order to facilitate the comparison, the dimensions of the plate for this analysis were chosen to be exactly the same as Maruyama's. The first seven natural frequencies of a test plate were calculated using the ADINA package. Table 4-1 contains a comparison of the calculated natural frequencies with Maruyama's results. The comparison shows that the natural frequencies were slightly overestimated by the finite element model relative to Maruyama's numerical predictions, but the difference is at most 2%. The agreement between the two sets of results is good, and on this basis the finite element model is assumed to be reliable.

Table 4-1. Comparison of the natural frequencies of an undamaged plate with Maruyama's numerical result

frequency (Hz)	f_1	f_2	f_3	f_4	f_5	f_6	f_7
Finite element results	326	587	728	964	1004	1319	1387
Maruyama's results	318	579	714	960	990	1315	1365
Difference in %	2	1	2	1	1	1	2

2. Comparison of calculated natural frequencies with experimental results

The finite element model was used to calculate the natural frequencies and modal shapes for each experimental case. The actual plate dimensions were used in this analysis, and the slot width for damaged plates was 5/64 inch. For each experimental case, a corresponding finite element analysis was carried out.

As an initial check of the experimental results, a comparison was made between experimental and numerical results for undamaged plates. Table 4-2 contains the first five natural frequencies obtained by both methods. In this table, the mean of the measured natural frequencies for three plates was used as the experimental result. As shown by Table 4-2, there is a good agreement, with differences of 3% or less, between experimental and numerical results.

Table 4-2. Comparison between experimental and numerical results for natural frequencies of undamaged plates

frequency	experimental results(H z)	numerical results(Hz)	difference in %
f_1	335	342	-2
f_2	631	617	3
f_3	749	765	-2
f_4	1024	1013	1
f_5	1089	1055	3

Table 4-3 contains the first five calculated natural frequencies for plates with horizontal slots, corresponding to the experimental results presented in Table 3-2.

Table 4-3. Calculated natural frequencies of a plate with horizontal slot

frequency(Hz)	2.0" slot	2.5" slot	3.0" slot
f_1	325	316	308
f_2	618	614	610
f_3	727	687	628
f_4	1017	1012	1000
f_5	1045	1042	1030

Table 4-4 contains the first five calculated natural frequencies for plates with 45 degree slots, corresponding to experimental results presented in Table 3-3.

Table 4-4. Calculated natural frequencies of a plate with 45 degree slot

frequency(Hz)	2.0" slot	2.5" slot	3.0" slot
f_1	325	318	311
f_2	605	588	556
f_3	744	720	698
f_4	967	938	915
f_5	1033	1033	1025

Table 4-5 contains the calculated natural frequencies for plates with vertical slots, corresponding to the experimental results presented in Table 3-4.

Table 4-5. Calculated natural frequencies of a plate with vertical slot (Hz)

frequency(Hz)	2.0" slot	2.5" slot	3.0" slot
f_1	329	324	316
f_2	599	576	517
f_3	659	757	725
f_4	1010	1003	946
f_5	961	932	897

Tables 4-6 through 4-8 compare relative changes in the natural frequencies between the experimental and numerical results for plates with horizontal, 45 degree, and vertical slots, respectively.

Table 4-6. Comparison of relative changes in the natural frequencies of a plate with a horizontal slot (%)

	2.0" slot		2.5" slot		3.0" slot	
	FEM[a]	MTM[b]	FEM	MTM	FEM	MTM
$\Delta f_1/f_1$	-5	-7	-8	-8	-10	-10
$\Delta f_2/f_2$	0	2	-1	1	- 1	0
$\Delta f_3/f_3$	-5	-6	-10	-11	-18	-20
$\Delta f_4/f_4$	0	0	-1	-1	-1	-3
$\Delta f_5/f_5$	-1	1	-1	1	-3	-1

[a]FEM Finite Element Model.
[b]MTM Modal Testing Method.

Table 4-7. Comparison of relative changes in the natural frequencies of a plate with a 45 degree slot (%)

	2.0" slot		2.5" slot		3.0" slot	
	FEM	MTM	FEM	MTM	FEM	MTM
$\Delta f_1/f_1$	-5	-8	-7	-9	-10	-10
$\Delta f_2/f_2$	-2	-4	-5	-8	-10	-15
$\Delta f_3/f_3$	-3	-3	-6	-5	- 9	- 6
$\Delta f_4/f_4$	-5	-6	-7	-8	-10	-10
$\Delta f_5/f_5$	-2	-4	-2	-5	-3	- 5

Table 4-8. Comparison of relative changes in the natural frequencies of a plate with a vertical slot (%)

	2.0" slot		2.5" slot		3.0" slot	
	FEM	MTM	FEM	MTM	FEM	MTM
$\Delta f_1/f_1$	-4	-2	-5	-4	-8	-6
$\Delta f_2/f_2$	-3	-5	-6	-8	-16	-17
$\Delta f_3/f_3$	-1	0	-1	-2	-5	-3
$\Delta f_4/f_4$	0	0	-1	0	-7	-4
$\Delta f_5/f_5$	-9	-11	-12	-13	-15	-15

The comparisons reveal that experimental and finite element results are in good agreement. In all but one case, the differences in the relative changes in natural frequencies are 3% or less. The conclusion is that both the natural frequencies measured by modal testing and predicted by the finite element method are reliable. The results also suggest that a near field microphone is a suitable response transducer for the experimental determination of natural frequencies.

3. Effects of slot length on the changes in natural frequency

Both the finite element estimates and the experimental results listed in Tables of 4-6 through 4-8 show that slot length has a significant influence on changes in natural frequency. Furthermore, the effects of slot length are not uniform for the five natural frequencies. Some of the natural frequencies are very sensitive to changes in slot

length, and some are relatively insensitive to changes in slot length. For example, the natural frequency f_3 decreases rapidly, with increasing slot length for the horizontal slot case. The decrease in f_3 goes from 6% to 20%, as slot length increases from 2.0 to 3.0 inches. On the other hand, the relative changes in the natural frequency f_1 are relatively insensitive to change in slot length. Similar behavior also occurs for other slot orientations. The results also indicate that in some cases higher natural frequencies are more sensitive to damage.

4. Effects of slot orientation on the changes in natural frequency

Three different slot orientations; horizontal, 45 degree, and vertical with respect to the base of the plate, were studied both experimentally and numerically. Relative changes in natural frequencies for each case were summarized in Tables 4-6 through 4-8. Table 4-9 contains a comparison of relative changes in natural frequencies of plates with 2.5 by 5/64 inch slots for three orientations. The results show that the orientation of the slot has a significant effect on changes in natural frequency. For instance, the natural frequency f_3 exhibited a large change for a horizontal slot, but changed very little for an identical vertical slot. There was also a considerable change in f_3 for a 45 degree slot. Careful examination of the results revealed relationships among the orientation, modal shapes, and changes in natural frequencies of the plates. Parts (a) through (f) of Figure 4-3 are sketches of the first five modal shapes of an undamaged plate that were obtained using the finite element method. In this figure the heavy

line represents the node line corresponding to the modal shape. The results reveal that when the slot is perpendicular to the node line of a modal shape, the natural frequency associated with the modal shape will have little change. On the other hand, if the slot coincides with the node line of a modal shape, the frequency corresponding to the modal shape will have a large reduction. When the slot is in a 45 degree direction with respect to the node line of a modal shape, the frequency may also have considerable change.

Table 4-9. Comparison of relative changes in the natural frequencies for a 2.5 in. slot at three orientations

	horizontal	45 degree	vertical
$\Delta f_1/f_1$	-8	-7	-5
$\Delta f_2/f_2$	-1	-5	-6
$\Delta f_3/f_3$	-10	-6	-1
$\Delta f_4/f_4$	-1	-7	-1
$\Delta f_5/f_5$	-1	-2	-12

5. Effects of slot width on natural frequency

In order to study the effect of slot width on the natural frequencies, four different slots having the same length and orientation, but different width, were simulated numerically. Centered, vertical slots were studied for 0.02, 0.05, 0.078, and 0.1719 inch slot widths.

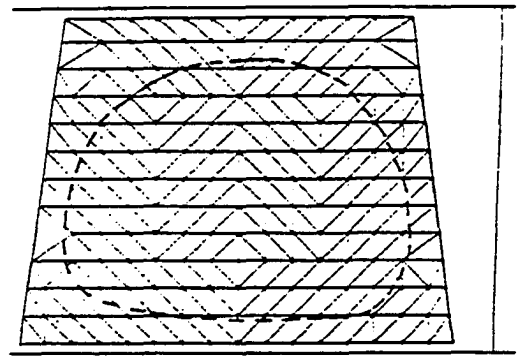

342 (Hz)

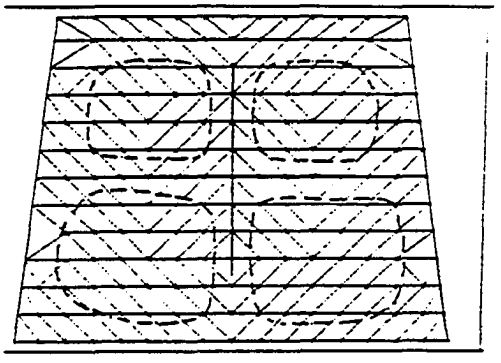

1013 (Hz)

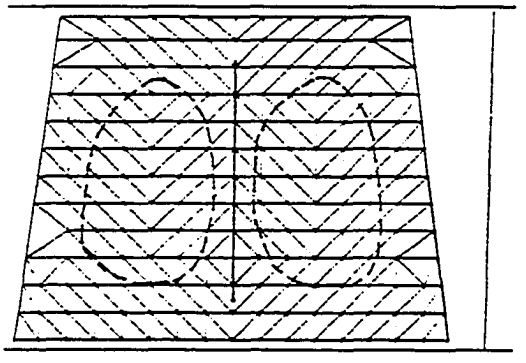

617 (Hz)

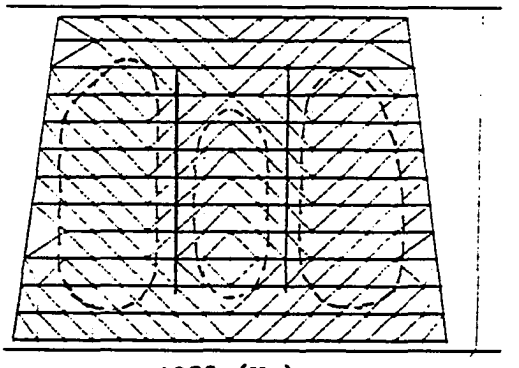

1055 (Hz)

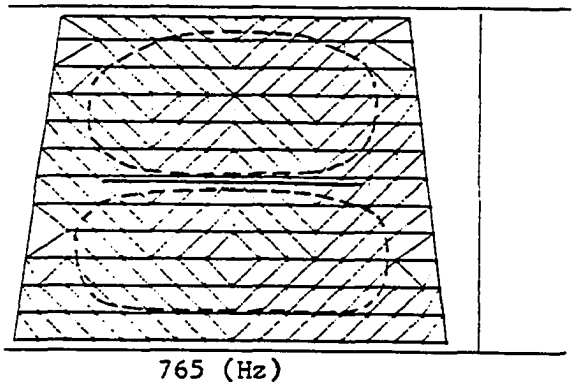

765 (Hz)

Figure 4-3. The first five modal shapes of an undamaged plate

Table 4-10 contains the calculated natural frequencies for plates with four different slot widths. The results shown reveal that when the slot width increases by a factor of 9 from 0.02 to 0.1719 in., relative changes in the predicted natural frequencies are less than 1 percent. This is true for even the most sensitive frequency, f_2. The results indicate that slot width has little effect on natural frequency for vertical slots, and it is assumed that similar results would be obtained for other slot orientations.

Table 4-10. Calculated natural frequencies of four plates with different slot widths

frequency	without slot	width of slot (in.) 0.02	0.05	0.078	0.1719
f_1	342	329	329	329	330
f_2	617	602	600	599	596
f_3	765	759	759	759	759
f_4	1013	1011	1011	1010	1006
f_5	1055	959	961	961	966
f_6	1386	1378	1378	1378	1377
f_7	1457	1428	1429	1429	1413

6. Changes in modal shapes

The modal shapes for each damaged plate were investigated numerically. Figures 4-4 (a) through (f) are sketches of the first five modal shapes of a plate with a 2.0 by 5/64 inch vertical slot. Figures 4-5 (a) through (f) are sketches of the modal shapes of a plate with a 3.0 by 5/64 inch 45 degree slot. Comparing Figs. 4-3, 4-4, and

4-5, reveals that the predicted modal shapes are almost unchanged for a 2.0 in. slot. For 3.0 a in. slot, the modal shapes also show little change. The presence of a centered slot appears to have little influence on the modal shapes, although it does affect the natural frequencies considerably.

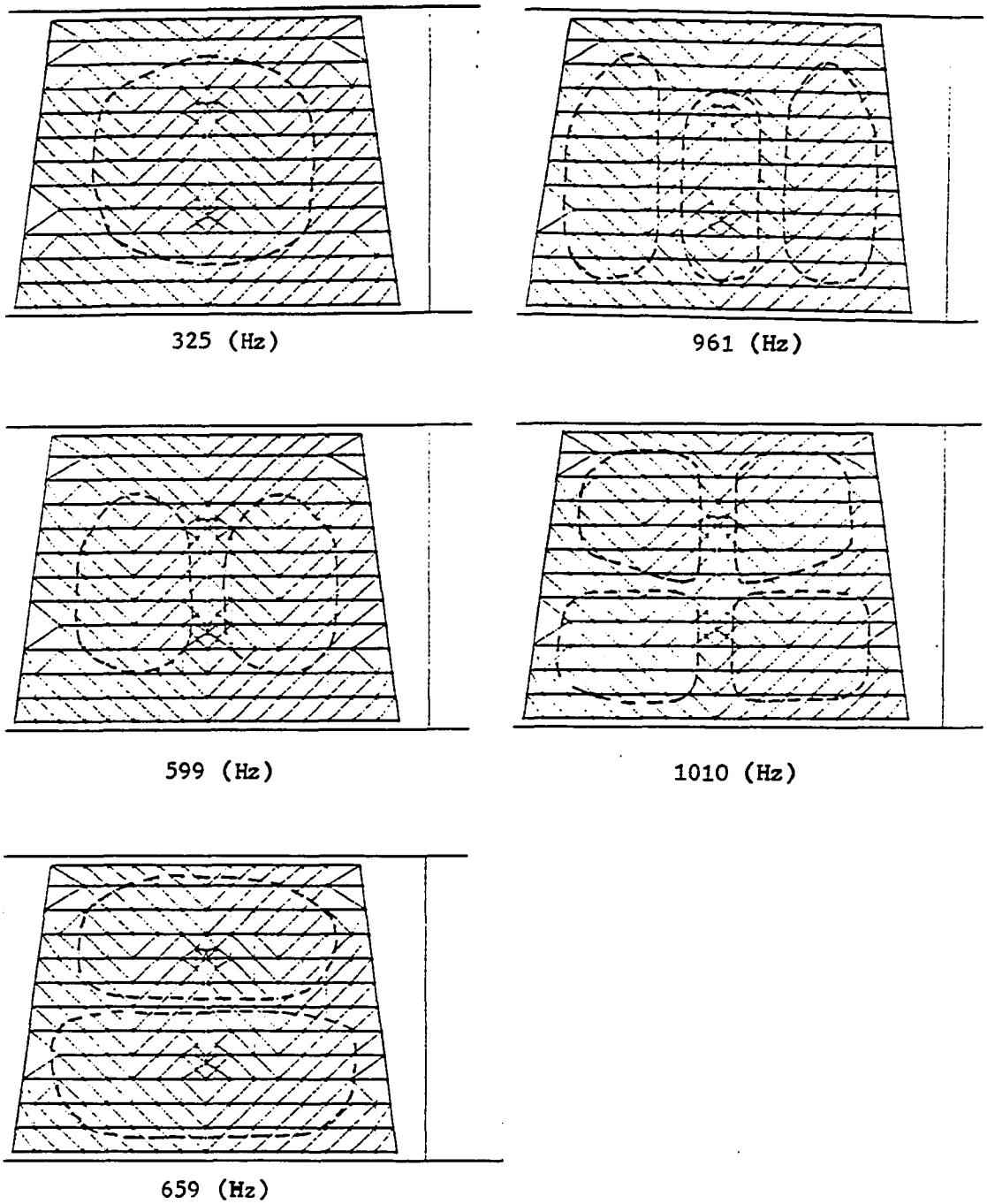

Figure 4-4. The first five modal shapes of a plate with a 2.0 in. vertical slot

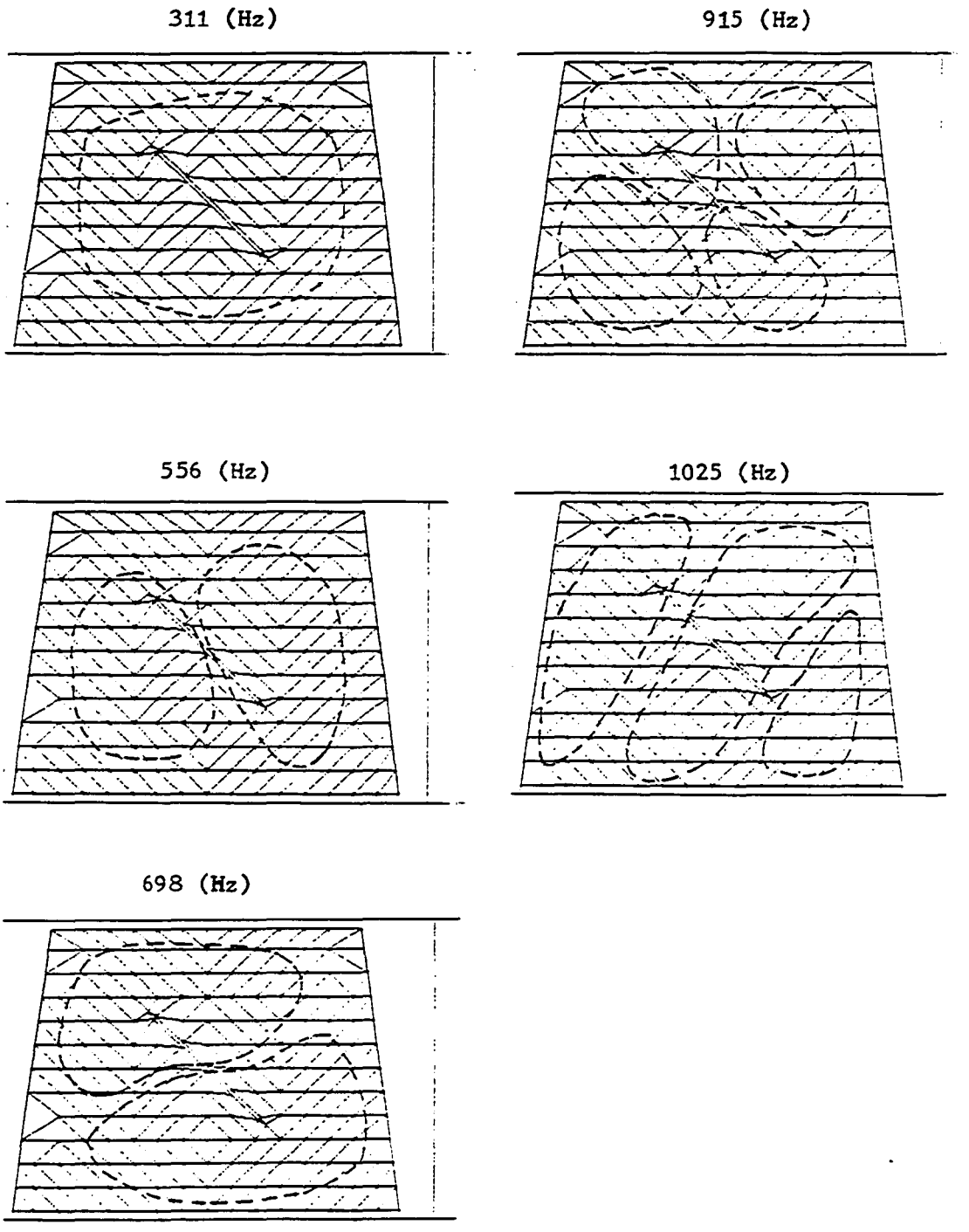

Figure 4-5. The sketch of modal shapes for plate with slot of 3.0" length at 45 degrees direction

V. CONCLUSIONS AND RECOMMENDATIONS

A. Conclusions

The objective of the research described in this dissertation was to investigate methods for the detection, location, and characterization of a flaw or damage in a structure or machine by modal analysis techniques. Damage considered in this work was restricted to narrow, rectangular slots in symmetric trapezoidal plates. Both modal testing and finite element methods were used to investigate changes in natural frequencies of a clamped trapezoidal plate for all combinations of three slot lengths and three slot orientations. In modal testing, an impulse hammer was used to excite the plate vibration, while a near field microphone was used to measure the response of the test plates. The finite element analysis was carried out using the ADINA finite element package. The changes in natural frequencies obtained by the two methods were in good agreement for all cases studied. Moreover, the numerical results agree well with Maruyama's work for an undamaged plate. The results suggest that impact vibrational analysis using a near field microphone as the response transducer can produce satisfactory experimental results. They also indicate that finite element analysis can be used to study the effects of damage on the change in natural frequencies.

The results contain a number of interesting features concerning the detection, location, and characterization of existing damage or flaws.

1. The presence of a slot can be detected from the shift in natural

frequency of the test structure or machine. Natural frequencies associated with some higher modes were found to be more sensitive to the presence of a slot.

2. Slot width has no significant effect on natural frequencies.
3. Slot length has a significant effect on natural frequencies. The influence of slot length on natural frequencies is not uniform. Depending upon the orientation and location of the slot, some of the natural frequencies may exhibit substantial reduction while others may show little change.
4. Slot orientation also has a significant effect on natural frequencies. The relative orientation of a nodal line with respect to the slot is an important parameter in determining the effect of a slot on natural frequency.
5. The presence of a slot has little effect on the modal shapes, although it does influence the natural frequencies considerably.
6. The presence of a slot can change the numerical order of natural frequencies associated with adjacent modes.

All of the features listed are useful for characterizing the damage or flaw from the measured frequency change. They also indicate that the modal analysis technique is a potential method for macroscopic non-destructive evaluation.

B. Recommendations

In the research reported here, all slot lengths investigated have been large compared to the plate thickness. Both experimental and numerical results suggest that it may be possible to detect a short slot. For detecting short slots, changes in higher frequencies need to be measured. The impact hammer used in this research may be too heavy to excite the higher frequency range. Other excitation methods such as swept-sine or limited bandwidth random excitation should be considered. The Zooming techniques may also be useful for improving resolution.

Finite element analysis for small damage may involve refinement of the mesh. That may increase computer time considerably. This problem can be solved by using Eq. (1-1) to estimate the change in natural frequency, recalling that Eq. (1-1) connects the change in natural frequency to the change in stiffness from knowledge of the modal shapes and mass matrix for the undamaged structure. By means of Eq. (1-1), the change in natural frequency for a damaged structure can be estimated by reforming the stiffness matrix without repeating the computationally intensive dynamic analysis.

Only rectangular slots were investigated in this research. In another preliminary investigation, a number of centered circular holes were simulated numerically. It was found that the changes in the first five natural frequencies were very small, about 2%, even for a 1.2 inch diameter hole. This result suggests that the shape of the damage may have considerable effect on the natural frequencies. Other types of

damage encountered in practice, including a variety shapes and combinations of shapes should be studied.

BIBLIOGRAPHY

1. Adams, R. D., Cawley, P., Pye, C., J., and Stone, B. J. "A Vibration Technique for Non-destructively Assessing the Integrity of Structures." Journal of Mechanical Engineering Science, 20, No. 2 (1978), 93-100.

2. Cawley, P. and Adams, R. D. "The Location of Defects in Structures from Measurements of Natural Frequencies." Journal of Strain Analysis, 14, No. 2 (1979), 49-57.

3. Crema, Balis L., Castellani, A., and Peroni, I. "Modal Tests on Composite Material Structures Application in Damage Detection." In Proc. 3rd IMAC, vol. II. Orlando, FL: Union College, 1985, pp. 708-713.

4. Tracy, John J., Dimas, David J., and Pardoen, Gerard C. "Advanced Composite Damage Detection Using Modal Analysis Techniques." In Proc. 2nd IMAC, vol. II. Orlando, FL: Union College, 1984, pp. 655-660.

5. Chondros, T. G. and Dimarogonas, A. D. "Identification of Cracks in Welded Joints of Complex Structures." Journal of Sound and Vibration, 69, No. 4 (1980), 531-538.

6. Yang, J. C. S., Chen, J., and Dagalakis, N. G. "Damage Detection in Offshore Structure by the Random Technique." Journal of Energy Resources Technology, 106 (March, 1984), 38-42.

7. Gudmundson, P. "Eigenfrequency Changes of Structures Due to Cracks, Notches or Other geometrical Changes." Journal of Mechanical Physics in Solids, 30, No. 5 (1982), 339-353.

8. Gudmundson, P. "The Dynamic Behaviour of Slender Structures with Cross-section Cracks." Journal of the Mechanics and Physics of Solids, 31, No. 4 (1983), 329-345.

9. Gudmundson, P. "Changes in Modal Parameters Resulting from Small Cracks." In Proc. 2nd IMAC, vol. I. Orlando, FL: Union College, 1984, pp. 690-697.

10. Maruyama, K., Ichinomiya, O., and Narita, Y. "Experimental Study of the Free Vibration of Clamped Trapezoidal Plates." Journal of Sound and Vibration, 88, No. 4 (1983), 523-534.

11. Kennedy, C. C. and Pancu, C. D. P. "Use of Vibration Measurement and Analysis." Journal of Aeronautical Sciences, 14, No. 11 (1947),

603-625.

12. Bishop, R. E. D. and Gladwell, G. M. L. "An Investigation into the Theory of Resonance Testing." Proc. Royal Society Phil. Trans., 255(A) (1963), 241-280.

13. Allemeng, R. J. "Experimental Modal Analysis Bibliography." In Proc. 3rd IMAC, vol. II. Orlando, FL: Union College, 1985, pp. 1084-1097.

14. Mitchell, L. D. and Mitchell, L. D. "Modal Analysis Bibliography - An Update 1980 - 1983." In Proc. 3rd IMCA, vol. II. Orlando, FL: Union College, 1985, pp. 1098-1114.

15. Richardson, Mark and Potter, Ron. "Identification of the Modal Parameters of an Elastic Structure from Measured Transfer Function Data." In Proc. 20th International Instrumentation Symposium, Albuquerque, N.M.: ISA, 1974, pp. 239-246.

16. Halvorsen, W. G., and Brown, D. L. "Impulse Technique for Structural Frequency Response Testing." Sound and Vibration, 11, No. 11 (1977), 8-21.

17. Ramsey, K. A. "Effective Measurement for Structural Dynamics Testing." Sound and Vibration, 10, No. 4 (1976), 18-31.

18. Ewins, D. J. Modal Testing: Theory and Practice. New York: John Wiley & Sons Inc., 1984.

19. Brown, D. L., Allemang, R. J., Zimmerman, R., and Mergeay, M. "Parameter Estimation Techniques for Modal Analysis." SAE paper No. 790221, 1979.

20. Salter, J. P. Steady State Vibration. Havant, Hampshire: Mason Press, 1969.

21. Hou, Z., Cheng, Y., Tong, Z., Sun, Y., and Lu, N. "Modal Parameter Identification from Multi-points Measured Data." In Proc. 3rd IMCA, vol. I. Orlando, FL: Union College, 1985, pp. 138-144.

22. Thomson, W. T. Theory of Vibration with Applications. 2nd edition. Englewood Cliffs, N. J.: Prentice - Hall, Inc., 1981.

23. Ewins, D. J. and Gleeson, P. T. "A Method for Modal Identification of Lightly Damped Structures." Journal of Sound and Vibration, 84, No. 1 (1982), 57-59.

24. Corelli, Dave and Brown, David L. "Impact Testing Considerations." In Proc. 2nd IMAC, vol. I. Orlando, FL: Union College, 1984, pp. 735-742.

25. Sohaney, R. C., and Nieters, J. M. "Proper Use of Weighting Functions for Impact Testing." In Proc. 3rd IMCA, vol. II. Orlando, FL: Union College, 1985, pp. 1102-1106.

26. Comstock, T. R., Javidinejad, M., Fleming, J. E., and Collins, R. L. "Use of the Microphone and Impact Hammer Windowing in Modal Testing." In Proc. Computer Aided Testing and Modal Analysis, SEM fall Conference, Milwankee, WI, 1984, pp. 55-60.

27. Cook, Robert D. Concepts and Applications of Finite Element Analysis. Second edition. New York: John Wiley & Sons, 1981.

28. ADINA Users Manual. ADINA Engineering Report number AE 81-1. ADINA Engineering, Inc., Watertown, Mass., Sept., 1981.

ACKNOWLEDGEMENTS

I would like to thank my major professor Dr. David K. Holger for his patience, encouragement, and sound guidance throughout this research. Thanks also go to my committee members Dr. Anna Mielnicka-Pate, Dr. Jeffrey C. Huston, Dr. Thomas R. Rogge, and Dr. Grover R. Brown for their support. The assistant of Mr. Thomas J. Elliott in preparing the experimental apparatus is also appreciated.

APPENDIX A. MEASURED FREQUENCY RESPONSE FUNCTION

Appendix A consists of two parts. Part A contains graphs of measured phase and magnitude of the frequency response function for plates with different horizontal slot lengths. Part B contains graphs of frequency response function measured at different points on a plate with a 2.5 by 5/64 in. vertical slot.

A. Measured Frequency Response Function of Plate with Various Horizontal Slot Lengths

Figures A-1 through A-4 show the measured phase and magnitude of the frequency response function for a plate without slot, and with a 2.0 inch, 2.5 inch, and 3.0 inch slot, respectively.

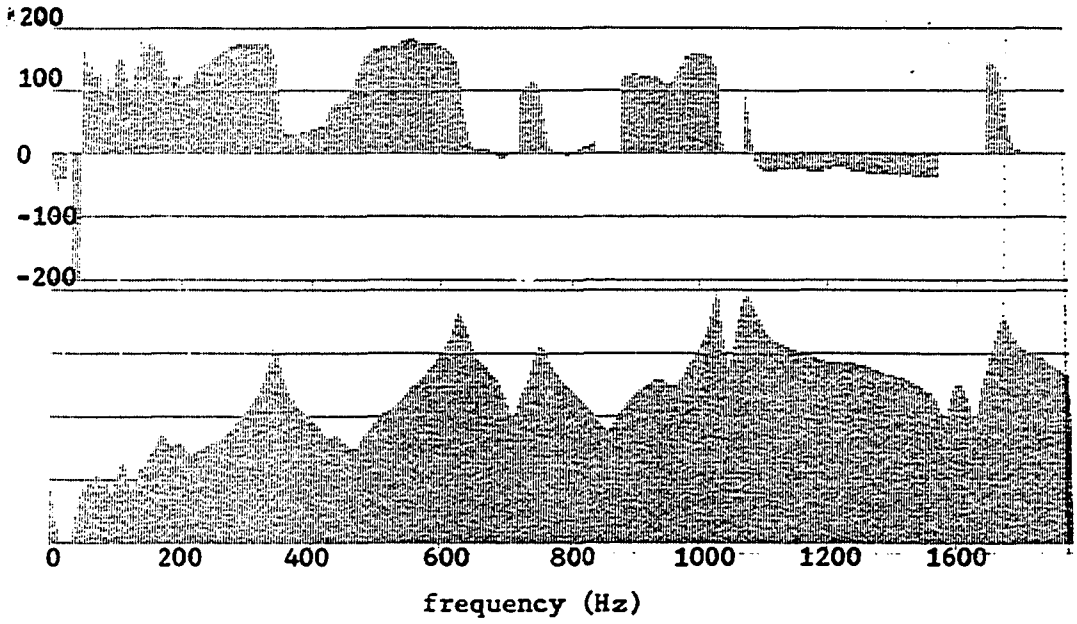

Figure A-1. Measured phase and magnitude of the frequency response function for an undamaged plate

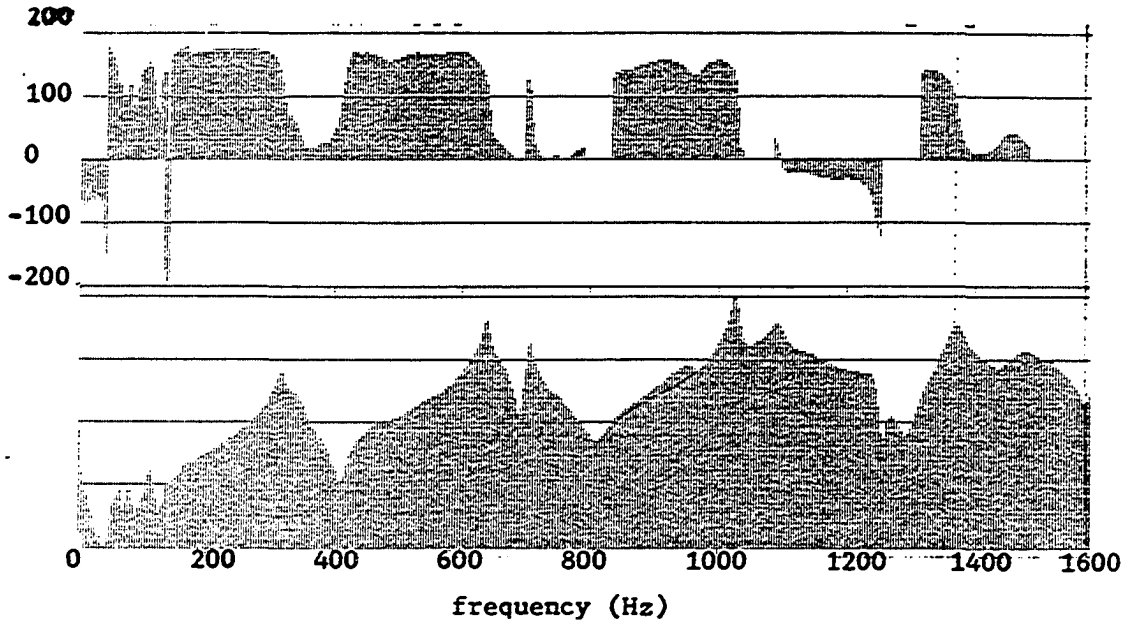

Figure A-2. Measured phase and magnitude of the frequency response function for a plate with a 2.0 by 5/64 in. horizontal slot

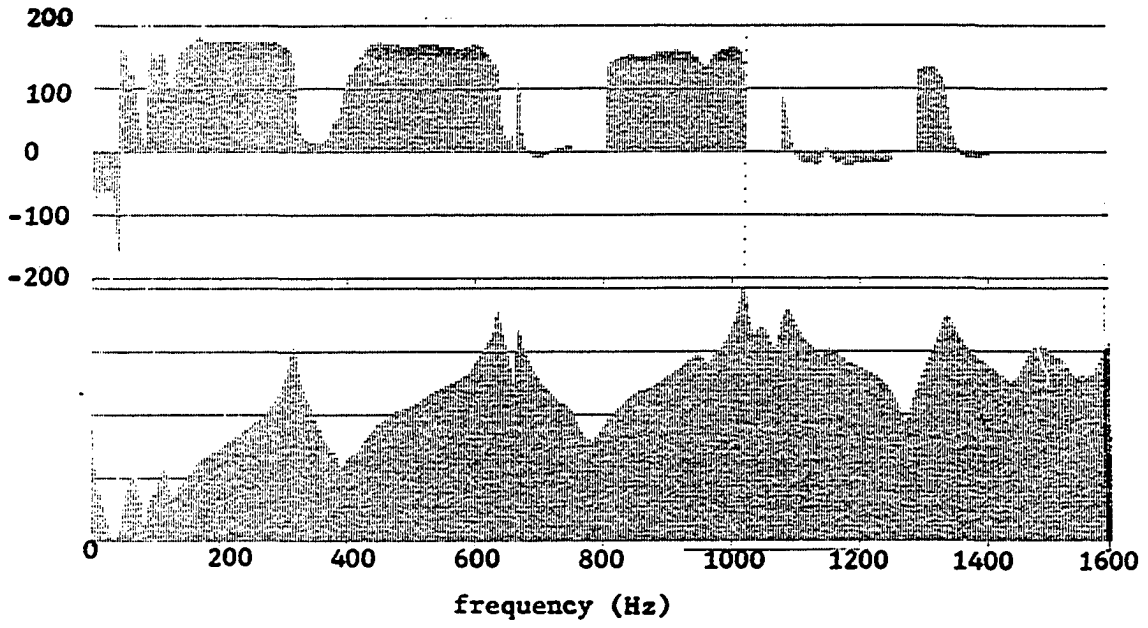

Figure A-3. Measured phase and magnitude of the frequency response function for a plate with a 2.5 by 5/64 in. horizontal slot

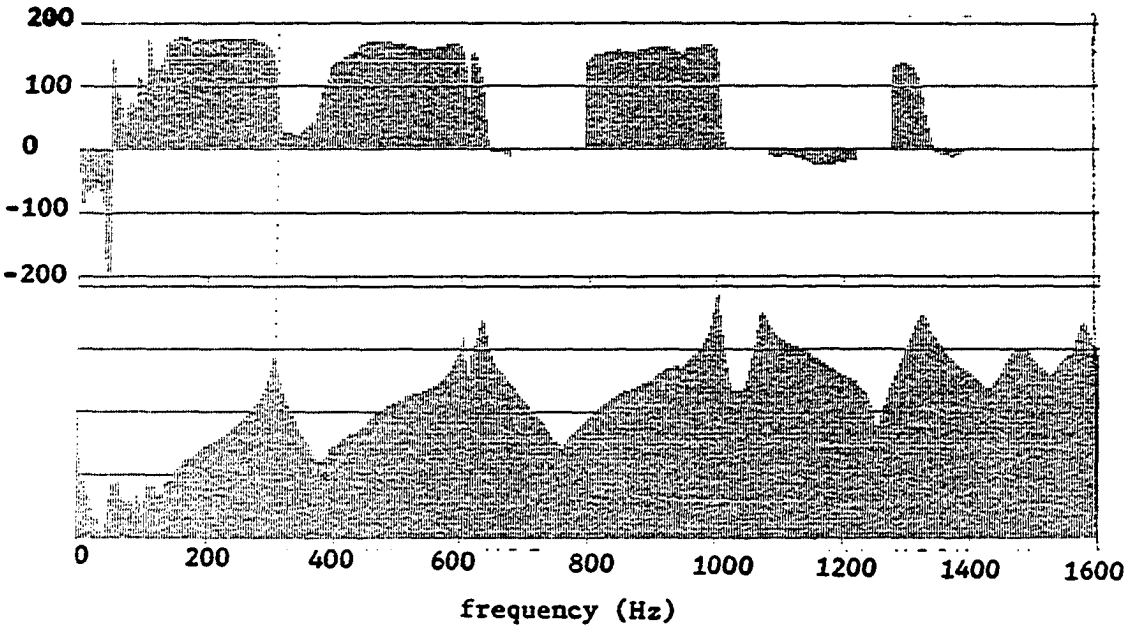

Figure A-4. Measured phase and magnitude of the frequency response function for a plate with a 3.0 by 5/64 in. horizontal slot

B. Frequency Response Function Measured at Different Points on a Plate with Vertical Slot

Figures A-5 through A-11 show the frequency response function measured at points 1 through 7 of Fig. 3-6 for a plate with a 2.5 by 5/64 in. vertical slot.

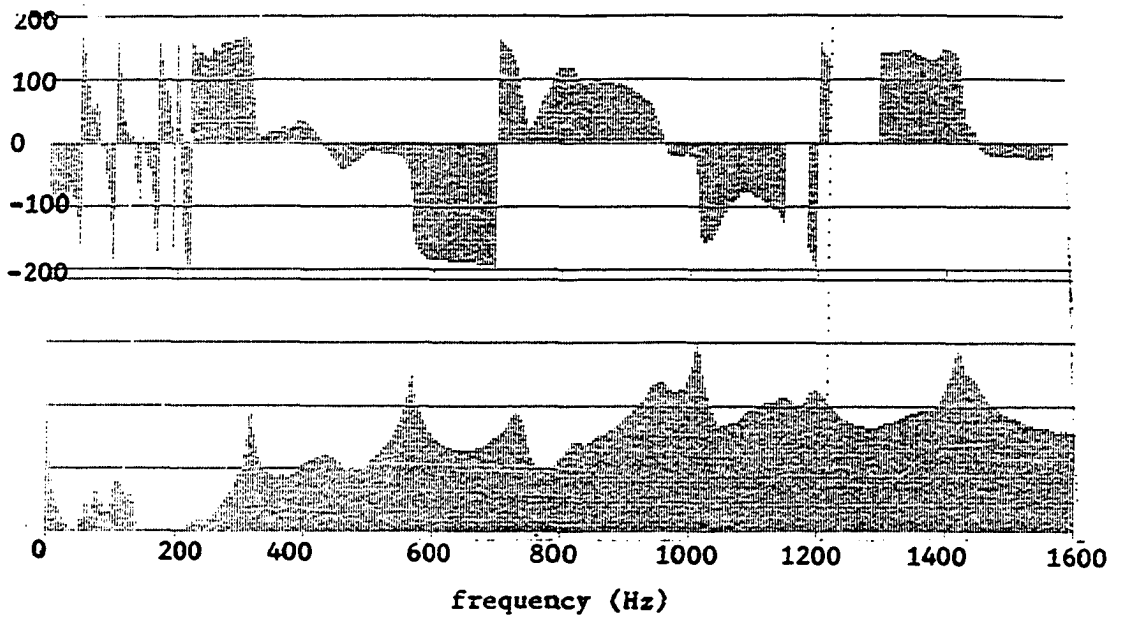

Figure A-5. Phase and magnitude of frequency response function measured at point No. 1

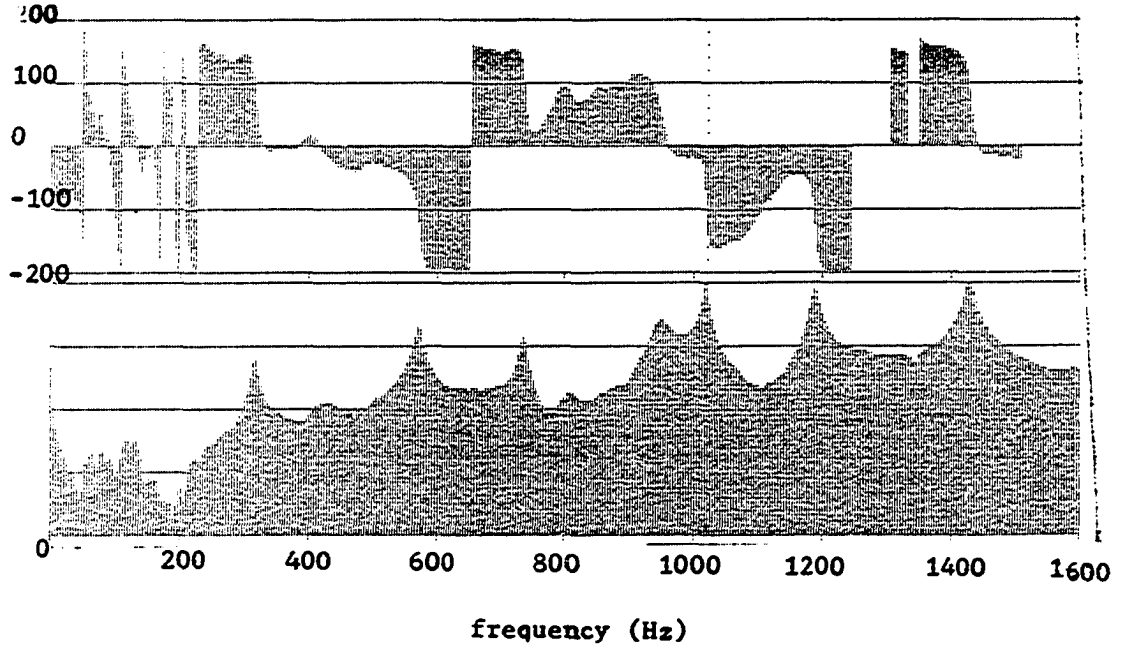

Figure A-6. Phase and magnitude of frequency response function measured at point No. 2

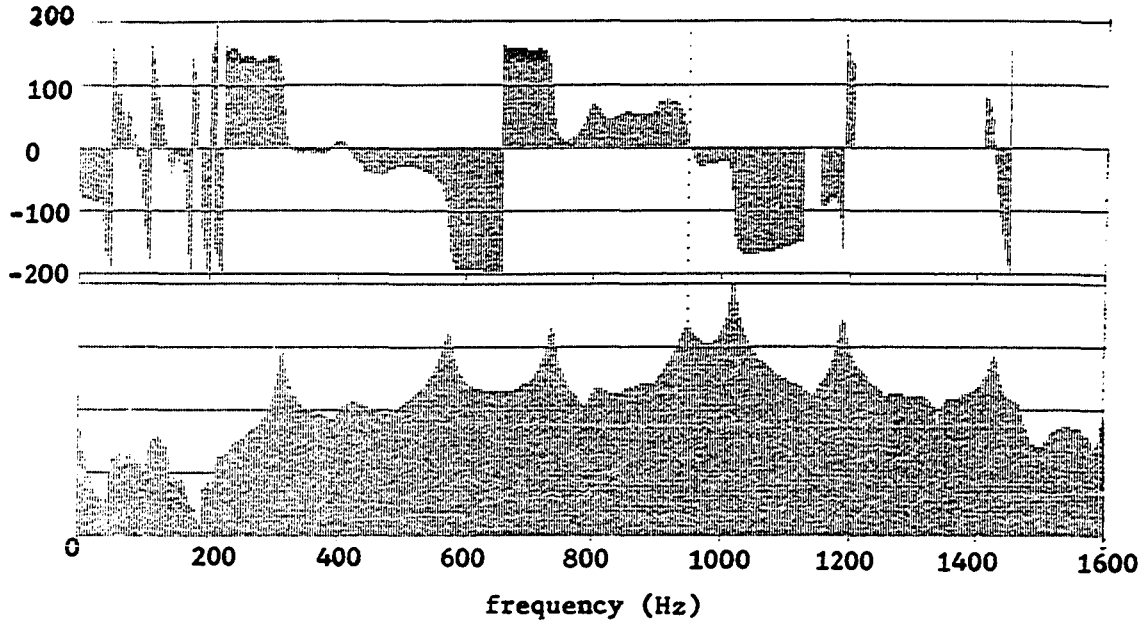

Figure A-7. Phase and magnitude of frequency response function measured at point No. 3

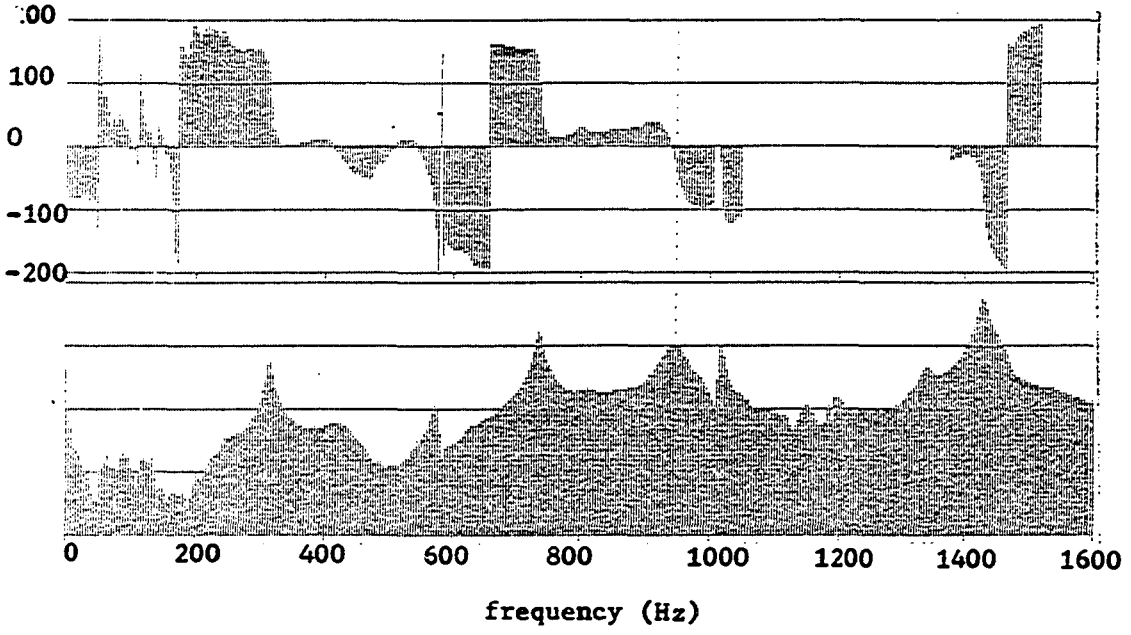

Figure A-8. Phase and magnitude of frequency response function measured at point No. 4

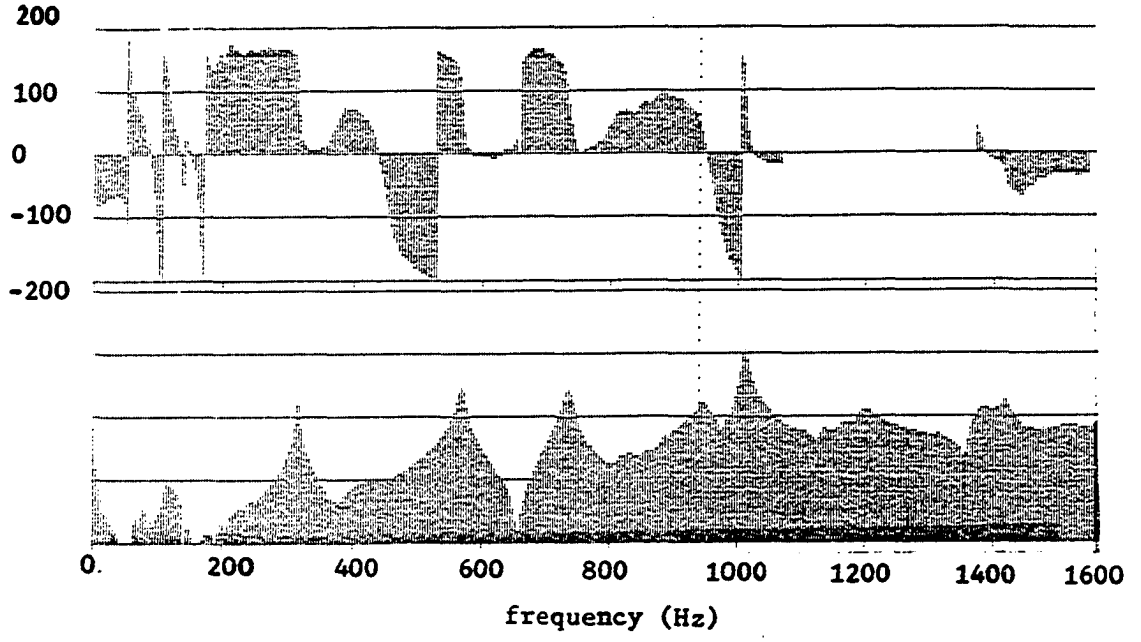

Figure A-9. Phase and magnitude of frequency response function measured at point No. 5

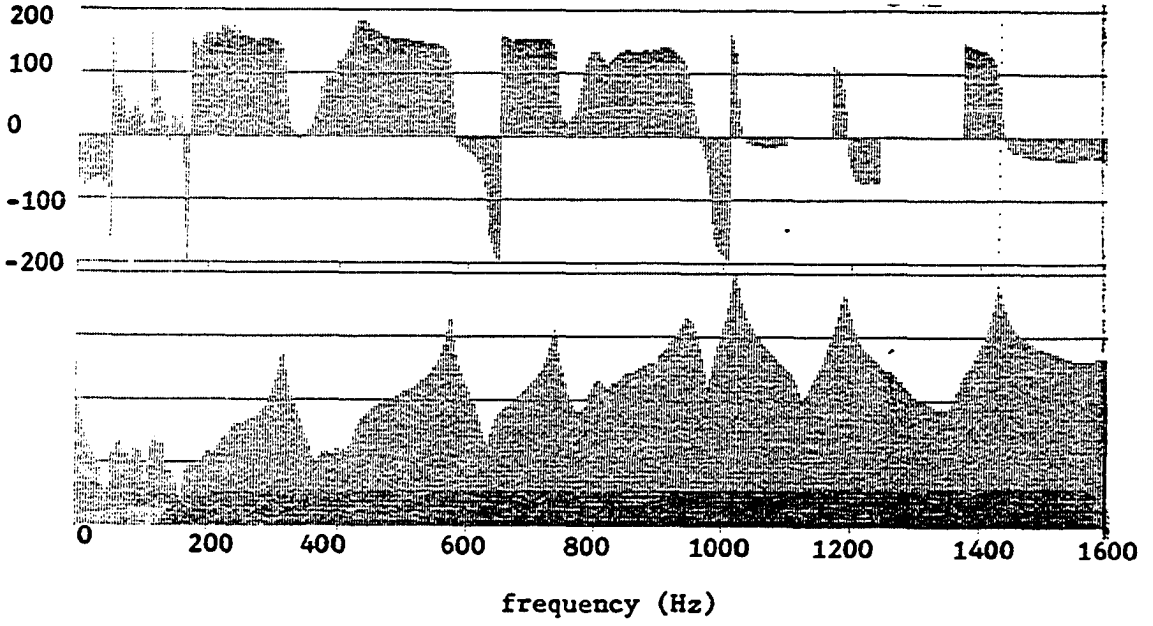

Figure A-10. Phase and magnitude of frequency response function measured at point No. 6

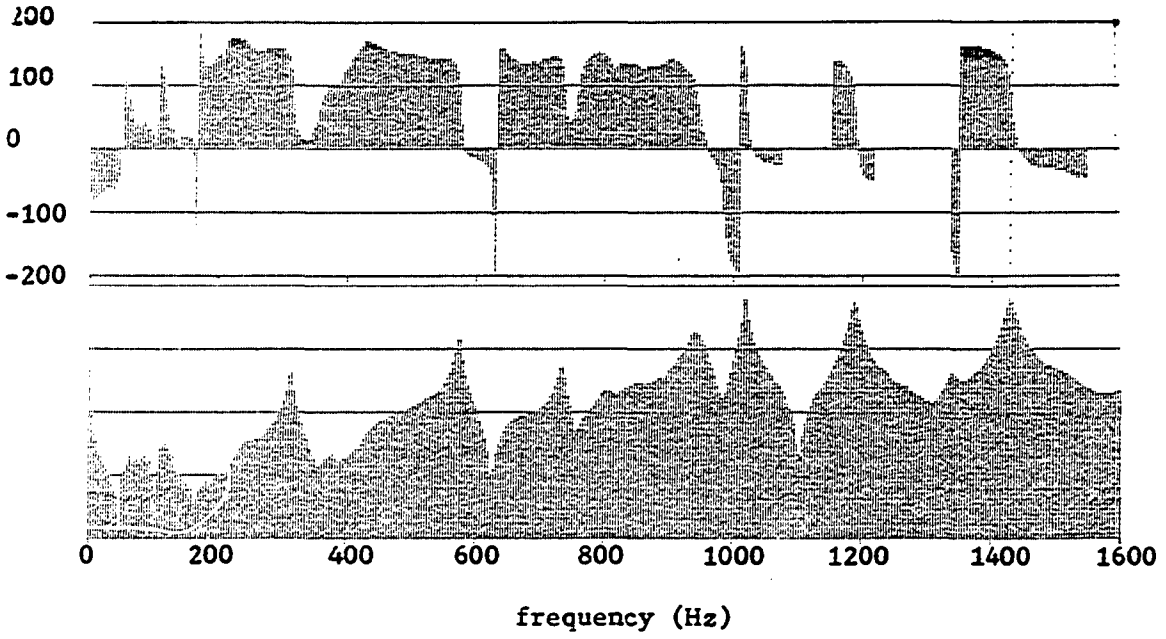

Figure A-11. Phase and magnitude of frequency response function measured at point No. 7

APPENDIX B. INPUT DATA SAMPLE

A. Input Data File

Appendix B is a listing of a input data file and calculated natural frequencies using the finite element package ADINA. This data file is for a plate with a 2.0 by 11/64 in. centered vertical slot.

```
C*********************************************************************
C***        ADINA INPUT DATA SAMPLE                                  *
C***        This is a input data list which shows the input format.  *
C***        This data file is for solving eigenvalue problem of a    *
C***        plate with 2.0 by 11/64 inch centered slot using three   *
C***        node plate element.  The total nodal number is 213, and  *
C***        element number is 365.                                   *
C***        The following is the input data file.                    *
C*********************************************************************
C***The following is the HEADING card
MODAL ANALYSIS OF PLATE WITH 2.0" BY 11/64 " VERTICAL SLOT
C***The following is the master control card No. 1.
C***For eigenvalue problem NSTE = 0, DT = TSTART = ANY positive
C***number.
  213000001   1         1    0    1.0    1.0          1
C***The following is master control card No. 2.  JNPORT = 1 means
C***that the porthole data file that is used for ADINA-plot is created.
                   1
C*** The following is master control card No. 3 which is for specifying
C***the loadings, for this problem all parameters are zero.

C***The following is mass and damping control card.  IMASS = 1 means
C***the lumped mass matrix is used.
    1
C***The following is frequency solution control card.
    1    1    7    0    7    1
C***The following is for time integration method.
    1    0       0.0              7
C***The following input is for non-linear analysis.
    0    0    1    0
C***Next card is the print-out control card.
    1    1    1    1    0         1
C***The following card is for creating porthole data file used for
C***ADINA-plot.
    1    1    1                          1    0    0
C***The following is the Block Definition Cards for print-out time
C***step (see III-3).
    1    1    1
C***The following card is Block Definition Cards for nodal
C***quantities print out (see III-4).
    1  213    1
C***The following two cards are for saving the response on porthole.
```

```
    1    1    1
    1    1    1
C***The following is time function control card, for eigenvalue
C***problem (NSTE= 0), all the parameters are zero.

C***The following group is NODAL POINT DATA CARDS.
    1    1    1    1    1    1    1  -3.9375  0.0       0.0
    2    1    1    1    1    1    1  -3.87236 0.5       0.0
    3    1    1    1    1    1    1  -3.80722 1.0       0.0
    4    1    1    1    1    1    1  -3.74211 1.5       0.0
    5    1    1    1    1    1    1  -3.6118  2.5       0.0
    6    1    1    1    1    1    1  -3.54666 3.0       0.0
    7    1    1    1    1    1    1  -3.48152 3.5       0.0
    8    1    1    1    1    1    1  -3.41638 4.0       0.0
    9    1    1    1    1    1    1  -3.35124 4.5       0.0
   10    1    1    1    1    1    1  -3.28610 5.0       0.0
   11    1    1    1    1    1    1  -3.22095 5.50000   0.0
   12    1    1    1    1    1    1  -3.16667 5.91667   0.0
   13    1    1    1    1    1    1  -3.50    0.0       0.0
   14    0    0    0    0    0    1   -3.5    0.5       0.0
   15    0    0    0    0    0    1   -3.5    1.0       0.0
   16    1    1    1    1    1    1   -3.0    0.0       0.0
   17    0    0    0    0    0    1   -3.0    0.5       0.0
   18    0    0    0    0    0    1   -3.0    1.0       0.0
   19    0    0    0    0    0    1   -3.0    1.5       0.0
   20    0    0    0    0    0    1   -3.0    2.0       0.0
   21    0    0    0    0    0    1   -3.0    2.5       0.0
   22    0    0    0    0    0    1   -3.0    3.0       0.0
   23    0    0    0    0    0    1   -3.0    3.5       0.0
   24    0    0    0    0    0    1   -3.0    4.0       0.0
   25    0    0    0    0    0    1   -3.0    4.5       0.0
   26    1    1    1    1    1    1   -2.5    0.0       0.0
   27    0    0    0    0    0    1   -2.5    0.5       0.0
   28    0    0    0    0    0    1   -2.5    1.0       0.0
   29    0    0    0    0    0    1   -2.5    1.5       0.0
   30    0    0    0    0    0    1   -2.5    2.0       0.0
   31    0    0    0    0    0    1   -2.5    2.5       0.0
   32    0    0    0    0    0    1   -2.5    3.0       0.0
   33    0    0    0    0    0    1   -2.5    3.5       0.0
   34    0    0    0    0    0    1   -2.5    4.0       0.0
   35    0    0    0    0    0    1   -2.5    4.5       0.0
   36    0    0    0    0    0    1   -2.5    5.0       0.0
   37    0    0    0    0    0    1   -2.5    5.5       0.0
   38    1    1    1    1    1    1   -2.5    5.91667   0.0
   39    1    1    1    1    1    1   -2.0    0.0       0.0
   40    0    0    0    0    0    1    -2.0   0.5       0.0
   41    0    0    0    0    0    1    -2.0   1.0       0.0
   42    0    0    0    0    0    1    -2.0   1.5       0.0
   43    0    0    0    0    0    1    -2.0   2.0       0.0
   44    0    0    0    0    0    1    -2.0   2.5       0.0
```

45	0	0	0	0	0	1	-2.0	3.0	0.0
46	0	0	0	0	0	1	-2.0	3.5	0.0
47	0	0	0	0	0	1	-2.0	4.0	0.0
48	0	0	0	0	0	1	-2.0	4.5	0.0
49	0	0	0	0	0	1	-2.0	5.0	0.0
50	0	0	0	0	0	1	-2.0	5.5	0.0
51	1	1	1	1	1	1	-2.0	5.91667	0.0
52	1	1	1	1	1	1	-1.5	0.0	0.0
53	0	0	0	0	0	1	-1.5	0.5	0.0
54	0	0	0	0	0	1	-1.5	1.0	0.0
55	0	0	0	0	0	1	-1.5	1.5	0.0
56	0	0	0	0	0	1	-1.5	2.0	0.0
57	0	0	0	0	0	1	-1.5	2.5	0.0
58	0	0	0	0	0	1	-1.5	3.0	0.0
59	0	0	0	0	0	1	-1.5	3.5	0.0
60	0	0	0	0	0	1	-1.5	4.0	0.0
61	0	0	0	0	0	1	-1.5	4.5	0.0
62	0	0	0	0	0	1	-1.5	5.0	0.0
63	0	0	0	0	0	1	-1.5	5.5	0.0
64	1	0	0	1	1	1	-1.5	5.91667	0.0
65	1	1	1	1	1	1	-1.0	0.0	0.0
66	0	0	0	0	0	1	-1.0	0.5	0.0
67	0	0	0	0	0	1	-1.0	1.0	0.0
68	0	0	0	0	0	1	-1.0	1.5	0.0
69	0	0	0	0	0	1	-1.0	4.5	0.0
70	0	0	0	0	0	1	-1.0	5.0	0.0
71	0	0	0	0	0	1	-1.0	5.5	0.0
72	1	1	1	1	1	1	-1.0	5.91667	0.0
73	1	1	1	1	1	1	-0.5	0.0	0.0
74	0	0	0	0	0	1	-0.5	0.5	0.0
75	0	0	0	0	0	1	-0.5	1.0	0.0
76	0	0	0	0	0	1	-0.5	1.5	0.0
77	0	0	0	0	0	1	-0.5	4.5	0.0
78	0	0	0	0	0	1	-0.5	5.0	0.0
79	0	0	0	0	0	1	-0.5	5.5	0.0
80	1	1	1	1	1	1	-0.5	5.91667	0.0
81	1	1	1	1	1	1	0.0	0.0	0.0
82	0	0	0	0	0	1	0.0	0.5	0.0
83	0	0	0	0	0	1	0.0	1.0	0.0
84	0	0	0	0	0	1	0.0	1.5	0.0
85	0	0	0	0	0	1	0.0	4.5	0.0
86	0	0	0	0	0	1	0.0	5.0	0.0
87	0	0	0	0	0	1	0.0	5.5	0.0
88	1	1	1	1	1	1	0.0	5.91667	0.0
89	1	1	1	1	1	1	0.5	0.0	0.0
90	0	0	0	0	0	1	0.5	0.5	0.0
91	0	0	0	0	0	1	0.5	1.0	0.0
92	0	0	0	0	0	1	0.5	1.5	0.0
93	0	0	0	0	0	1	0.5	4.5	0.0
94	0	0	0	0	0	1	0.5	5.0	0.0

95	0	0	0	0	0	1	0.5	5.5	0.0
96	1	1	1	1	1	1	0.5	5.91667	0.0
97	1	1	1	1	1	1	1.0	0.0	0.0
98	0	0	0	0	0	1	1.0	0.5	0.0
99	0	0	0	0	0	1	1.0	1.0	0.0
100	0	0	0	0	0	1	1.0	1.5	0.0
101	0	0	0	0	0	1	1.0	4.5	0.0
102	0	0	0	0	0	1	1.0	5.0	0.0
103	0	0	0	0	0	1	1.0	5.5	0.0
104	1	1	1	1	1	1	1.0	5.91667	0.0
105	1	1	1	1	1	1	1.5	0.0	0.0
106	0	0	0	0	0	1	1.5	0.5	0.0
107	0	0	0	0	0	1	1.5	1.0	0.0
108	0	0	0	0	0	1	1.5	1.5	0.0
109	0	0	0	0	0	1	1.5	2.0	0.0
110	0	0	0	0	0	1	1.5	2.5	0.0
111	0	0	0	0	0	1	1.5	3.0	0.0
112	0	0	0	0	0	1	1.5	3.5	0.0
113	0	0	0	0	0	1	1.5	4.0	0.0
114	0	0	0	0	0	1	1.5	4.5	0.0
115	0	0	0	0	0	1	1.5	5.0	0.0
116	0	0	0	0	0	1	1.5	5.5	0.0
117	1	0	0	1	1	1	1.5	5.91667	0.0
118	1	1	1	1	1	1	2.0	0.0	0.0
119	0	0	0	0	0	1	2.0	0.5	0.0
120	0	0	0	0	0	1	2.0	1.0	0.0
121	0	0	0	0	0	1	2.0	1.5	0.0
122	0	0	0	0	0	1	2.0	2.0	0.0
123	0	0	0	0	0	1	2.0	2.5	0.0
124	0	0	0	0	0	1	2.0	3.0	0.0
125	0	0	0	0	0	1	2.0	3.5	0.0
126	0	0	0	0	0	1	2.0	4.0	0.0
127	0	0	0	0	0	1	2.0	4.5	0.0
128	0	0	0	0	0	1	2.0	5.0	0.0
129	0	0	0	0	0	1	2.0	5.5	0.0
130	1	1	1	1	1	1	2.0	5.91667	0.0
131	1	1	1	1	1	1	2.5	0.0	0.0
132	0	0	0	0	0	1	2.5	0.5	0.0
133	0	0	0	0	0	1	2.5	1.0	0.0
134	0	0	0	0	0	1	2.5	1.5	0.0
135	0	0	0	0	0	1	2.5	2.0	0.0
136	0	0	0	0	0	1	2.5	2.5	0.0
137	0	0	0	0	0	1	2.5	3.0	0.0
138	0	0	0	0	0	1	2.5	3.5	0.0
139	0	0	0	0	0	1	2.5	4.0	0.0
140	0	0	0	0	0	1	2.5	4.5	0.0
141	0	0	0	0	0	1	2.5	5.0	0.0
142	0	0	0	0	0	1	2.5	5.5	0.0
143	1	1	1	1	1	1	2.5	5.91667	0.0
144	1	1	1	1	1	1	3.0	0.0	0.0

145	0	0	0	0	0	1	3.0	0.5	0.0
146	0	0	0	0	0	1	3.0	1.0	0.0
147	0	0	0	0	0	1	3.0	1.5	0.0
148	0	0	0	0	0	1	3.0	2.0	0.0
149	0	0	0	0	0	1	3.0	2.5	0.0
150	0	0	0	0	0	1	3.0	3.0	0.0
151	0	0	0	0	0	1	3.0	3.5	0.0
152	0	0	0	0	0	1	3.0	4.0	0.0
153	0	0	0	0	0	1	3.0	4.5	0.0
154	1	1	1	1	1	1	3.50	0.0	0.0
155	0	0	0	0	0	1	3.5	0.5	0.0
156	0	0	0	0	0	1	3.5	1.0	0.0
157	1	1	1	1	1	1	3.9375	0.0	0.0
158	1	1	1	1	1	1	3.87236	0.5	0.0
159	1	1	1	1	1	1	3.80722	1.0	0.0
160	1	1	1	1	1	1	3.74211	1.5	0.0
161	1	1	1	1	1	1	3.67694	2.0	0.0
162	1	1	1	1	1	1	3.6118	2.5	0.0
163	1	1	1	1	1	1	3.54666	3.0	0.0
164	1	1	1	1	1	1	3.48152	3.5	0.0
165	1	1	1	1	1	1	3.41638	4.0	0.0
166	1	1	1	1	1	1	3.35124	4.5	0.0
167	1	1	1	1	1	1	3.28610	5.0	0.0
168	1	1	1	1	1	1	3.22095	5.50000	0.0
169	1	1	1	1	1	1	3.16667	5.91667	0.0
170	0	0	0	0	0	1	-1.0	2.0	0.0
171	0	0	0	0	0	1	-1.0	2.5	0.0
172	0	0	0	0	0	1	-1.0	3.0	0.0
173	0	0	0	0	0	1	-1.0	3.5	0.0
174	0	0	0	0	0	1	-1.0	4.0	0.0
175	0	0	0	0	0	1	-0.5	2.0	0.0
176	0	0	0	0	0	1	-0.5	2.5	0.0
177	0	0	0	0	0	1	-0.5	3.0	0.0
178	0	0	0	0	0	1	-0.5	3.5	0.0
179	0	0	0	0	0	1	-0.5	4.0	0.0
180	0	0	0	0	0	1	-0.085938	2.0	0.0
181	0	0	0	0	0	1	-0.085938	2.5	0.0
182	0	0	0	0	0	1	-0.085938	3.0	0.0
183	0	0	0	0	0	1	-0.085938	3.5	0.0
184	0	0	0	0	0	1	-0.085938	4.0	0.0
185	0	0	0	0	0	1	0.5	2.0	0.0
186	0	0	0	0	0	1	0.5	2.5	0.0
187	0	0	0	0	0	1	0.5	3.0	0.0
188	0	0	0	0	0	1	0.5	3.5	0.0
189	0	0	0	0	0	1	0.5	4.0	0.0
190	0	0	0	0	0	1	1.0	2.0	0.0
191	0	0	0	0	0	1	1.0	2.5	0.0
192	0	0	0	0	0	1	1.0	3.0	0.0
193	0	0	0	0	0	1	1.0	3.5	0.0
194	0	0	0	0	0	1	1.0	4.0	0.0

```
  195    0    0    0    0    0    1    0.0     4.15       0.0
  196    0    0    0    0    0    1    0.0     1.85       0.0
  197    0    0    0    0    0    1   -0.2     1.7        0.0
  198    0    0    0    0    0    1    0.2     1.7        0.0
  199    0    0    0    0    0    1   -0.2     2.0        0.0
  200    0    0    0    0    0    1 0.0859375  2.0        0.0
  201    0    0    0    0    0    1 0.0859375  2.5        0.0
  202    0    0    0    0    0    1 0.0859375  3.0        0.0
  203    0    0    0    0    0    1 0.0859375  3.5        0.0
  204    0    0    0    0    0    1 0.0859375  4.0        0.0
  205    0    0    0    0    0    1    0.2     2.0        0.0
  206    0    0    0    0    0    1   -0.2     2.2        0.0
  207    0    0    0    0    0    1    0.2     2.2        0.0
  208    0    0    0    0    0    1   -0.2     3.8        0.0
  209    0    0    0    0    0    1    0.2     3.8        0.0
  210    0    0    0    0    0    1   -0.2     4.0         0.0
  211    0    0    0    0    0    1    0.2     4.0        0.0
  212    0    0    0    0    0    1   -0.2     4.2        0.0
  213    0    0    0    0    0    1    0.2     4.2        0.0
C***The following is initial condition control card

C***The following is element group control card.
   6 365   0                                                1
C***The following two cards are the material property data.
    1 0.0002588
   10.6E06    0.325
C***The following group is the element data cards.
    1    4    2
    1    1    1                    0.0397
    1   13    2
    2    1    1                    0.0397
    2   13   14
    3    1    1                    0.0397
    2   14    3
    4    1    1                    0.0397
    3   14   15
    5    1    1                    0.0397
    3   15    4
    6    1    1                    0.0397
   13   16   14
    7    1    1                    0.0397
   14   16   17
    8    1    1                    0.0397
   14   17   15
    9    1    1                    0.0397
   15   17   18
   10    1    1                    0.0397
   15   18   19
   11    1    1                    0.0397
    4   15   19
```

12	1	1	0.0397
4	19	20	
13	1	1	0.0397
4	20	5	
14	1	1	0.0397
5	20	21	
15	1	1	0.0397
5	21	6	
16	1	1	0.0397
6	21	22	
17	1	1	0.0397
6	22	7	
18	1	1	0.0397
7	22	23	
19	1	1	0.0397
7	23	8	
20	1	1	0.0397
8	23	24	
21	1	1	0.0397
8	24	9	
22	1	1	0.0397
9	24	25	
23	1	1	0.0397
9	25	10	
24	1	1	0.0397
10	25	36	
25	1	1	0.0397
10	36	37	
26	1	1	0.0397
10	37	11	
27	1	1	0.0397
11	37	12	
28	1	1	0.0397
12	37	38	
29	1	1	0.0397
16	26	17	
30	1	1	0.0397
17	26	27	
31	1	1	0.0397
17	27	18	
32	1	1	0.0397
18	27	28	
33	1	1	0.0397
18	28	19	
34	1	1	0.0397
19	28	29	
35	1	1	0.0397
19	29	20	
36	1	1	0.0397
20	29	30	

37	1	1	0.0397
20	30	21	
38	1	1	0.0397
21	30	31	
39	1	1	0.0397
21	31	22	
40	1	1	0.0397
22	31	32	
41	1	1	0.0397
22	32	23	
42	1	1	0.0397
23	32	33	
43	1	1	0.0397
23	33	24	
44	1	1	0.0397
24	33	34	
45	1	1	0.0397
24	34	25	
46	1	1	0.0397
25	34	35	
47	1	1	0.0397
25	35	36	
48	1	1	0.0397
26	39	27	
49	1	1	0.0397
27	39	40	
50	1	1	0.0397
27	40	28	
51	1	1	0.0397
28	40	41	
52	1	1	0.0397
28	41	29	
53	1	1	0.0397
29	41	42	
54	1	1	0.0397
29	42	30	
55	1	1	0.0397
30	42	43	
56	1	1	0.0397
30	43	31	
57	1	1	0.0397
31	43	44	
58	1	1	0.0397
31	44	32	
59	1	1	0.0397
32	44	45	
60	1	1	0.0397
32	45	33	
61	1	1	0.0397
33	45	46	

62	1	1	0.0397
33	46	34	
63	1	1	0.0397
34	46	47	
64	1	1	0.0397
34	47	35	
65	1	1	0.0397
35	47	48	
66	1	1	0.0397
35	48	36	
67	1	1	0.0397
36	48	49	
68	1	1	0.0397
36	49	37	
69	1	1	0.0397
37	49	50	
70	1	1	0.0397
37	50	38	
71	1	1	0.0397
38	50	51	
72	1	1	0.0397
39	52	40	
73	1	1	0.0397
40	52	53	
74	1	1	0.0397
40	53	41	
75	1	1	0.0397
41	53	54	
76	1	1	0.0397
41	54	42	
77	1	1	0.0397
42	54	55	
78	1	1	0.0397
42	55	43	
79	1	1	0.0397
43	55	56	
80	1	1	0.0397
43	56	44	
81	1	1	0.0397
44	56	57	
82	1	1	0.0397
44	57	45	
83	1	1	0.0397
45	57	58	
84	1	1	0.0397
45	58	46	
85	1	1	0.0397
46	58	59	
86	1	1	0.0397
46	59	47	

87	1	1	0.0397
47	59	60	
88	1	1	0.0397
47	60	48	
89	1	1	0.0397
48	60	61	
90	1	1	0.0397
48	61	49	
91	1	1	0.0397
49	61	62	
92	1	1	0.0397
49	62	50	
93	1	1	0.0397
50	62	63	
94	1	1	0.0397
50	63	51	
95	1	1	0.0397
51	63	64	
96	1	1	0.0397
52	65	53	
97	1	1	0.0397
53	65	66	
98	1	1	0.0397
53	66	54	
99	1	1	0.0397
54	66	67	
100	1	1	0.0397
54	67	55	
101	1	1	0.0397
55	67	68	
102	1	1	0.0397
61	69	62	
103	1	1	0.0397
62	69	70	
104	1	1	0.0397
62	70	63	
105	1	1	0.0397
63	70	71	
106	1	1	0.0397
63	71	64	
107	1	1	0.0397
64	71	72	
108	1	1	0.0397
65	73	66	
109	1	1	0.0397
66	73	74	
110	1	1	0.0397
66	74	67	
111	1	1	0.0397
67	74	75	

112	1	1	0.0397
67	75	68	
113	1	1	0.0397
68	75	76	
114	1	1	0.0397
69	77	70	
115	1	1	0.0397
70	77	78	
116	1	1	0.0397
70	78	71	
117	1	1	0.0397
71	78	79	
118	1	1	0.0397
72	71	79	
119	1	1	0.0397
72	79	80	
120	1	1	0.0397
73	81	74	
121	1	1	0.0397
74	81	82	
122	1	1	0.0397
75	74	82	
123	1	1	0.0397
75	82	83	
124	1	1	0.0397
76	75	83	
125	1	1	0.0397
76	83	84	
126	1	1	0.0397
78	77	85	
127	1	1	0.0397
78	85	86	
128	1	1	0.0397
79	78	86	
129	1	1	0.0397
79	86	87	
130	1	1	0.0397
80	79	87	
131	1	1	0.0397
80	87	88	
132	1	1	0.0397
81	89	90	
133	1	1	0.0397
82	81	90	
134	1	1	0.0397
82	90	91	
135	1	1	0.0397
83	82	91	
136	1	1	0.0397
83	91	92	

137	1	1	0.0397
84	83	92	
138	1	1	0.0397
85	93	94	
139	1	1	0.0397
86	85	94	
140	1	1	0.0397
86	94	95	
141	1	1	0.0397
87	86	95	
142	1	1	0.0397
87	95	96	
143	1	1	0.0397
88	87	96	
144	1	1	0.0397
89	97	98	
145	1	1	0.0397
90	89	98	
146	1	1	0.0397
90	98	99	
147	1	1	0.0397
91	90	99	
148	1	1	0.0397
91	99	100	
149	1	1	0.0397
92	91	100	
150	1	1	0.0397
93	101	102	
151	1	1	0.0397
94	93	102	
152	1	1	0.0397
94	102	103	
153	1	1	0.0397
95	94	103	
154	1	1	0.0397
95	103	104	
155	1	1	0.0397
96	95	104	
156	1	1	0.0397
97	105	106	
157	1	1	0.0397
98	97	106	
158	1	1	0.0397
98	106	107	
159	1	1	0.0397
99	98	107	
160	1	1	0.0397
99	107	108	
161	1	1	0.0397
100	99	108	

162	1	1	0.0397
101	114	115	
163	1	1	0.0397
101	115	102	
164	1	1	0.0397
102	115	116	
165	1	1	0.0397
102	116	103	
166	1	1	0.0397
103	116	117	
167	1	1	0.0397
104	103	117	
168	1	1	0.0397
105	118	119	
169	1	1	0.0397
106	105	119	
170	1	1	0.0397
106	119	120	
171	1	1	0.0397
107	106	120	
172	1	1	0.0397
107	120	121	
173	1	1	0.0397
108	107	121	
174	1	1	0.0397
108	121	122	
175	1	1	0.0397
109	108	122	
176	1	1	0.0397
109	122	123	
177	1	1	0.0397
110	109	123	
178	1	1	0.0397
110	123	124	
179	1	1	0.0397
111	110	124	
180	1	1	0.0397
111	124	125	
181	1	1	0.0397
112	111	125	
182	1	1	0.0397
112	125	126	
183	1	1	0.0397
113	112	126	
184	1	1	0.0397
113	126	127	
185	1	1	0.0397
114	113	127	
186	1	1	0.0397
114	127	128	

187	1	1	0.0397
115	114	128	
188	1	1	0.0397
115	128	129	
189	1	1	0.0397
116	115	129	
190	1	1	0.0397
116	129	130	
191	1	1	0.0397
117	116	130	
192	1	1	0.0397
118	131	132	
193	1	1	0.0397
119	118	132	
194	1	1	0.0397
119	132	133	
195	1	1	0.0397
120	119	133	
196	1	1	0.0397
120	133	134	
197	1	1	0.0397
121	120	134	
198	1	1	0.0397
121	134	135	
199	1	1	0.0397
122	121	135	
200	1	1	0.0397
122	135	136	
201	1	1	0.0397
123	122	136	
202	1	1	0.0397
123	136	137	
203	1	1	0.0397
124	123	137	
204	1	1	0.0397
124	137	138	
205	1	1	0.0397
125	124	138	
206	1	1	0.0397
125	138	139	
207	1	1	0.0397
126	125	139	
208	1	1	0.0397
126	139	140	
209	1	1	0.0397
127	126	140	
210	1	1	0.0397
127	140	141	
211	1	1	0.0397
128	127	141	

212	1	1	0.0397
128	141	142	
213	1	1	0.0397
129	128	142	
214	1	1	0.0397
129	142	143	
215	1	1	0.0397
130	129	143	
216	1	1	0.0397
131	144	145	
217	1	1	0.0397
132	131	145	
218	1	1	0.0397
132	145	146	
219	1	1	0.0397
133	132	146	
220	1	1	0.0397
133	146	147	
221	1	1	0.0397
134	133	147	
222	1	1	0.0397
134	147	148	
223	1	1	0.0397
135	134	148	
224	1	1	0.0397
135	148	149	
225	1	1	0.0397
136	135	149	
226	1	1	0.0397
136	149	150	
227	1	1	0.0397
137	136	150	
228	1	1	0.0397
137	150	151	
229	1	1	0.0397
138	137	151	
230	1	1	0.0397
138	151	152	
231	1	1	0.0397
139	138	152	
232	1	1	0.0397
139	152	153	
233	1	1	0.0397
140	139	153	
234	1	1	0.0397
141	140	153	
235	1	1	0.0397
141	153	167	
236	1	1	0.0397
141	167	142	

237	1	1	0.0397
142	167	168	
238	1	1	0.0397
142	168	169	
239	1	1	0.0397
143	142	169	
240	1	1	0.0397
144	154	155	
241	1	1	0.0397
145	144	155	
242	1	1	0.0397
145	155	156	
243	1	1	0.0397
146	145	156	
244	1	1	0.0397
147	146	156	
245	1	1	0.0397
154	157	158	
246	1	1	0.0397
155	154	158	
247	1	1	0.0397
155	158	159	
248	1	1	0.0397
156	155	159	
249	1	1	0.0397
156	159	160	
250	1	1	0.0397
147	156	160	
251	1	1	0.0397
147	160	161	
252	1	1	0.0397
148	147	161	
253	1	1	0.0397
148	161	162	
254	1	1	0.0397
149	148	162	
255	1	1	0.0397
149	162	163	
256	1	1	0.0397
149	163	150	
257	1	1	0.0397
150	163	164	
258	1	1	0.0397
151	150	164	
259	1	1	0.0397
151	164	165	
260	1	1	0.0397
152	151	165	
261	1	1	0.0397
152	165	166	

262	1	1	0.0397
153	152	166	
263	1	1	0.0397
153	166	167	
264	1	1	0.0397
55	68	170	
265	1	1	0.0397
56	55	170	
266	1	1	0.0397
56	170	171	
267	1	1	0.0397
56	57	171	
268	1	1	0.0397
57	171	172	
269	1	1	0.0397
58	57	172	
270	1	1	0.0397
58	172	173	
271	1	1	0.0397
59	58	173	
272	1	1	0.0397
59	173	174	
273	1	1	0.0397
60	59	174	
274	1	1	0.0397
69	60	174	
275	1	1	0.0397
61	60	69	
276	1	1	0.0397
68	76	175	
277	1	1	0.0397
170	68	175	
278	1	1	0.0397
170	175	176	
279	1	1	0.0397
171	170	176	
280	1	1	0.0397
171	176	177	
281	1	1	0.0397
172	171	177	
282	1	1	0.0397
172	177	178	
283	1	1	0.0397
173	172	178	
284	1	1	0.0397
179	173	178	
285	1	1	0.0397
174	173	179	
286	1	1	0.0397
77	174	179	

```
287    1    1                0.0397
 69  174   77
288    1    1                0.0397
 76  197  175
289    1    1                0.0397
175  197  199
290    1    1                0.0397
175  206  176
291    1    1                0.0397
176  206  181
292    1    1                0.0397
176  181  182
293    1    1                0.0397
177  176  182
294    1    1                0.0397
183  177  182
295    1    1                0.0397
178  177  183
296    1    1                0.0397
208  178  183
297    1    1                0.0397
179  178  208
298    1    1                0.0397
 77  179  212
299    1    1                0.0397
 77  212   85
300    1    1                0.0397
198   92  185
301    1    1                0.0397
205  198  185
302    1    1                0.0397
207  185  186
303    1    1                0.0397
201  207  186
304    1    1                0.0397
202  201  186
305    1    1                0.0397
202  186  187
306    1    1                0.0397
203  202  187
307    1    1                0.0397
203  187  188
308    1    1                0.0397
209  203  188
309    1    1                0.0397
209  188  189
310    1    1                0.0397
213  189   93
311    1    1                0.0397
 85  213   93
```

312	1	1	0.0397
92	100	185	
313	1	1	0.0397
185	100	190	
314	1	1	0.0397
186	185	190	
315	1	1	0.0397
186	190	191	
316	1	1	0.0397
187	186	191	
317	1	1	0.0397
187	191	192	
318	1	1	0.0397
188	187	192	
319	1	1	0.0397
188	192	193	
320	1	1	0.0397
189	188	193	
321	1	1	0.0397
189	193	194	
322	1	1	0.0397
93	189	194	
323	1	1	0.0397
93	194	101	
324	1	1	0.0397
100	108	190	
325	1	1	0.0397
190	108	109	
326	1	1	0.0397
191	190	109	
327	1	1	0.0397
191	109	110	
328	1	1	0.0397
192	191	110	
329	1	1	0.0397
192	110	111	
330	1	1	0.0397
192	111	193	
331	1	1	0.0397
193	111	112	
332	1	1	0.0397
194	193	112	
333	1	1	0.0397
194	112	113	
334	1	1	0.0397
101	194	113	
335	1	1	0.0397
101	113	114	
336	1	1	0.0397
76	84	197	

337	1	1	0.0397
84	92	198	
338	1	1	0.0397
197	84	196	
339	1	1	0.0397
196	84	198	
340	1	1	0.0397
199	197	196	
341	1	1	0.0397
205	196	198	
342	1	1	0.0397
180	199	196	
343	1	1	0.0397
180	196	200	
344	1	1	0.0397
200	196	205	
345	1	1	0.0397
206	175	199	
346	1	1	0.0397
206	199	180	
347	1	1	0.0397
180	181	206	
348	1	1	0.0397
201	200	207	
349	1	1	0.0397
207	200	205	
350	1	1	0.0397
207	205	185	
351	1	1	0.0397
208	183	184	
352	1	1	0.0397
204	203	209	
353	1	1	0.0397
179	208	210	
354	1	1	0.0397
210	208	184	
355	1	1	0.0397
204	209	211	
356	1	1	0.0397
209	189	211	
357	1	1	0.0397
179	210	212	
358	1	1	0.0397
212	210	184	
359	1	1	0.0397
212	184	195	
360	1	1	0.0397
184	204	195	
361	1	1	0.0397
204	213	195	

```
  362    1    1                0.0397
  204  213  195
  363    1    1                0.0397
  213  211  189
  364    1    1                0.0397
   85  212  195
  365    1    1                0.0397
   85  195  213
C***The last input data is the frequency calculation card.
C*** All the parameter are zero for this problem.

STOP
```

****

B. The Calculated Natural Frequencies

FREQUENCIES

FREQUENCY NUMBER	FREQUENCY (RAD/SEC)	FREQUENCY (CYCLES/SEC)
1	0.2075E+04	0.3302E+03
2	0.3742E+04	0.5955E+03
3	0.4767E+04	0.7588E+03
4	0.6068E+04	0.9658E+03
5	0.6322E+04	0.1006E+04
6	0.8652E+04	0.1377E+04
7	0.8878E+04	0.1413E+04